IOP Publishing Plasma Physics and Controlled Fusion

Plasma Phys. Control. Fusion **58** (2016) 045024 (16pp) doi:10.1088/0741-3335/58/4/045024

Manifestations of the geodesic acoustic mode driven by energetic ions in tokamaks

Ya I Kolesnichenko[1], V V Lutsenko[1], Yu V Yakovenko[1], B S Lepiavko[1], B Grierson[2], W W Heidbrink[3] and R Nazikian[2]

[1] Institute for Nuclear Research, Prospekt Nauky 47, Kyiv 03680, Ukraine
[2] Princeton Plasma Physics Laboratory, Princeton, NJ 08540, USA
[3] University of California-Irvine, Irvine, CA 92697, USA

E-mail: yk@kinr.kiev.ua

Received 10 September 2015, revised 18 January 2016
Accepted for publication 5 February 2016
Published 1 March 2016

Abstract

Effects of the energetic-ion-driven Geodesic Acoustic modes (GAM and E-GAM) on the toroidally passing energetic ions and the concomitant change of the neutron yield of beam-plasma fusion reactions in tokamaks are considered. It is shown that due to large perturbations of the plasma density, the resonant energetic ions driving the instability can be considerably slowed down for a few tens of the particle transit periods, which is much less than the collisional slowing down time. The time of the collisionless slowing down is actually determined by the period of the particle motion within the resonance island arising because of the GAM / E-GAM. Being trapped in the island, the resonant particles can not only lose their energy but also gain it. One more effect of GAMs is the flattening on the distribution function of the resonant particles. Due to conservation of the canonical angular momentum during a GAM / E-GAM instability, the change of the particle energy is accompanied by a radial displacement of the resonant particle for a distance up to the poloidal Larmor radius of energetic ions. The particles are displaced inwards or outwards, depending on the direction of their motion along the magnetic field. Expressions describing the change of the neutron yield due to GAM modes are derived. It is found that the distortion of the velocity distribution of the resonant particles can lead to a considerable drop of the neutron emission even when effects of the particle radial displacement are small. The developed theory is applied to an E-GAM experiment on the DIII-D tokamak. Relations for the period of the motion within the resonance island of passing (both well passing and marginally passing) particles and the width of the resonance of the energetic particles with GAM modes and low-frequency Alfvén modes are derived.

Keywords: tokamak, energetic ions, geodesic acoustic mode, neutron emission

(Some figures may appear in colour only in the online journal)

1. Introduction

An oscillation homogeneous in the toroidal direction (the toroidal mode number $n = 0$), named Geodesic Acoustic Mode (GAM), was predicted to exist in toroidal plasmas by Winsor *et al* as long ago as in 1968 [1]. This mode was actually a solution of a continuum equation, i.e. it was a radially local solution. In many years after Winsor's prediction, it turned out that strongly localized oscillating zonal flows with the GAM features play an important role, regulating turbulent transport in toroidal plasmas [2, 3]. About 10 years ago, the $n = 0$ mode was observed in the JET tokamak [4, 5]. This mode was excited by energetic ions and named the Global Geodesic Acoustic Mode (G-GAM). Its frequency lied above the maximum of the GAM continuum and, in contrast to the Winsor solution, was not purely electrostatic. Wings of the magnetic perturbation reached the plasma edge and were detected by Mirnov coils. The epithet 'global' reflected the presence of these wings. However, the perturbation amplitude in the wings was small, the region with much larger amplitude

was rather narrow. More recently, a new $n = 0$ mode associated with energetic ions was observed in the DIII-D tokamak [6]. Measurements of the density fluctuation by beam emission spectroscopy (BES) showed that the mode was really wide, about a third of the plasma radius. Theoretical study confirmed the existence of the modes with this structure [7]. The studies in [6, 7] gave grounds for referring to the mode as E-GAM, i.e. Energetic-particle-induced GAM mode, because its frequency was less than the GAM frequency and determined by the transit frequency of the energetic ions. The mode considered in [7] was purely electrostatic. Like in [1–3], it had poloidally symmetric (the poloidal mode number $m = 0$) scalar potential of the perturbed electric field and asymmetric ($m = 1$) perturbed particle density. Bursts of the E-GAM instability driven by counter-injected energetic ions resulted in large (10–15%) drops of the neutron emission. These drops indicated the expulsion of the injected ions from the plasma core and, possibly, their loss (neutrons were produced mainly by the beam-plasma fusion reaction) [6]. Later DIII-D experiments have given a direct evidence of the influence of the E-GAM instability on the deterioration of the confinement of injected ions [8].

The GAM modes can be considered as electrostatic, and harmonics of the scalar potential of the electric field with $m \neq 0$ are negligible when β (the ratio of the plasma pressure to the magnetic field pressure) is sufficiently low, satisfying the condition $\beta_s \equiv c_s^2/v_A^2 < (8q^2)^{-1}$, where c_s is the sound velocity, v_A is the Alfvén velocity, and q is the tokamak safety factor [9, 10]. This was the case in the mentioned DIII-D experiment where $\beta \sim 0.4\%$ [6]. Therefore, the perturbed electric field in low-β plasmas and, in particular, in the DIII-D experiment can be approximated as $\tilde{\boldsymbol{E}} = (\tilde{E}_r, 0, 0)$ (tilde labels perturbations). This means that the radial component of the $\tilde{\boldsymbol{E}} \times \boldsymbol{B}$ drift vanishes ($\boldsymbol{B}$ is the equilibrium magnetic field). For this reason, a widespread point of view is that GAM / E-GAM does not affect the energetic ion transport and that the only direct effect of GAM / E-GAM on the energetic ions is the change of their pitch angles (which can lead to the transformation of passing ions to trapped ones and a concomitant increase of the particle radial displacement). However, as shown in [11], there is a direct mechanism of the transport of energetic ions across the magnetic field. This mechanism is associated with the decrease of the energy of fast ions driving the GAM instability, as explained below: The GAM mode conserves the canonical angular momentum of the energetic ions (P_ϕ) and their magnetic moment (μ_p). The same magnitudes are conserved in the absence of GAMs, but then, in addition, the particle energy ($\mathcal{E}$) is conserved. Therefore, in the absence of GAMs the equation $P_\phi(r, \theta, \mu_p, \mathcal{E}) = \text{const}$ determines the closed orbits in the (r, θ) plane (r and θ are the radial coordinate and poloidal coordinate, respectively). The presence of a GAM mode changes the energy of particles which are in the resonance with the mode. This makes the orbits unclosed.

In this paper, we consider the GAM-induced transport in more details, using another approach. In contrast to [11], a numerical solution of a single particle motion in the GAM field is carried out. Relationships for the resonance width are derived. The change of the neutron emission due to the GAM-induced transport of beam ions is evaluated. Like in [7], the analysis is carried out in the assumption that the mode is purely electrostatic.

Note that saying 'GAM mode' we mean only discrete eigenmodes, i.e. the modes having finite radial structure, rather than continuum modes considered in [1–3] and in many other works. These modes are excited by energetic ions, so that the only difference between the considered GAM modes and E-GAMs is that the existence and the frequency of E-GAMs are determined not only by the plasma but also by the energetic ions. For this reason, we often refer to both GAM and E-GAM as the GAM modes.

The structure of the paper is the following. Equations describing the behaviour of resonant passing ions in a tokamak magnetic field in the presence of the GAM electric field are solved and analysed in section 2. In addition, in this section the dependencies of the particle displacement and its energy change caused by the GAM instability on the mode amplitude are analysed. Section 3 deals with the influence of GAM modes on the neutron emission associated with beam-plasma fusion reactions. In section 3.1, expressions describing the change of the neutron yield in the case when the number of fast ions is conserved are obtained. In section 3.2 they are generalized to include the description of the marginally passing particles, which is of importance in connection with the mentioned DIII-D experiment. In this section the calculations relevant to this experiment are carried out. The results of the work are summarized in section 4. Appendix A contains the derivation of the width of the resonance of fast ions interacting with GAM modes or low-frequency Alfvén modes (whose frequency is small compared to the ion gyrofrequency) and the period of particle motion inside the resonance island, which uses a Hamiltonian formalism. Both well-passing ions and marginally passing ions are considered. Resonances which can provide the interaction of the the GAM / E-GAM modes with the particles are considered in appendix B. Finally, effects of the plasma temperature and toroidal rotation on the rate of D–D fusion reaction in the beam-plasma system are considered in appendix C.

2. Motion and change of the energy of resonant ions in the GAM field

In this section we consider effects of the GAM / E-GAM field on the passing ions. For simplicity, we restrict ourselves to a consideration of well-passing particles. Limits of applicability of this approach will be discussed in sections 3.2 and appendix A.

Let us take the mode electric field in the form $\tilde{E}_r = \hat{E} \sin \omega t$, where $\hat{E} \equiv \hat{E}(r) = -\mathrm{d}\Phi_{m=0,n=0}/\mathrm{d}r$, r is defined by $\psi_T = 0.5\kappa_e \bar{B} r^2$, ψ_T is the toroidal magnetic flux, κ_e is the elongation of the plasma cross section. In this field, the ion guiding centre motion is governed by the following equations:

$$\kappa_e \dot{r} = -v_D \sin\theta, \quad \dot{\theta} = \omega_t - \omega_D \cos\theta + \omega_E \sin\omega t,$$
$$\dot{\mathcal{E}} = e\dot{r}\hat{E} \sin\omega t, \qquad (1)$$

where ω_t is the transit frequency, ω_E is the frequency of the particle poloidal motion due to the $\hat{\boldsymbol{E}} \times \boldsymbol{B}$ drift, $\omega_D = v_D/(\kappa_e r)$, v_D is the velocity of the toroidal drift, dot over letters means the time derivative. Assuming that the mode amplitude is sufficiently small, we can make the transit time averaging. Then

$$\langle \dot{r} \rangle = -\frac{v_D}{\kappa_e \tau_t} \oint \frac{d\theta}{\dot{\theta}} \sin\theta \approx v_D \frac{\omega_E}{\kappa_e |\omega_t|} \oint \frac{d\theta}{2\pi} \sin\theta \sin\left[\omega t(\theta)\right], \tag{2}$$

$$\langle \dot{\mathcal{E}} \rangle = -e\hat{E} \frac{v_D}{\kappa_e} \oint \frac{d\theta}{2\pi} \sin\theta \sin\left[\omega t(\theta)\right], \tag{3}$$

where $\langle \ldots \rangle$ means the transit time averaging, $\tau_t = 2\pi/|\omega_t|$ is the transit period. It follows from (2) that, in general, $\langle \sin\theta \rangle \neq 0$ due to the presence of the GAM field and, thus, $\langle \dot{r} \rangle \neq 0$. Comparing (2) and (3), we obtain:

$$e\hat{E}\langle \dot{r} \rangle = -\sigma_v \frac{\omega_E}{|\omega_t|} \langle \dot{\mathcal{E}} \rangle, \tag{4}$$

where $\sigma_v = \operatorname{sgn} v_\parallel$, $v_\parallel$ is the particle velocity along the magnetic field. We observe that $\langle \dot{r} \rangle \neq 0$ when $\langle \dot{\mathcal{E}} \rangle \neq 0$ and vice versa. Because fast ions driving the instability give their energy to the mode, their energy decreases, $\langle \dot{\mathcal{E}} \rangle < 0$. Therefore, taking into account that $\omega_E \propto -\hat{E}$, we conclude from (4) that these ions move outwards in the case of counter injection ($\sigma_v < 0$) and inwards in the contrary case ($\sigma_v > 0$).

Note that the energy of a single ion interacting resonantly with the GAM mode does not necessarily decreases. To see it, we note that fast ions interact with GAMs through the resonance $\omega = |\omega_t|$ and that in this case $\theta \approx \omega t + \theta_0$ (due to small ω_E). Therefore, we can write the integral in (3) as

$$J(\omega = |\omega_t|) \equiv \oint \frac{d\theta}{2\pi} \sin\theta \sin\left[\omega t(\theta)\right] = \oint \frac{d\theta}{2\pi} \sin\theta \sin(\theta - \theta_0) = \frac{1}{2}\cos\theta_0. \tag{5}$$

It follows from (5) and (3) that, depending on θ_0, the mode-particle interaction leads either to the decrease of the particle energy or to its increase (provided that $\theta_0 \neq \frac{\pi}{2} + l\pi$, with $l = 1, 2, 3...$). This is not surprising: in the phase space $(\mathcal{E}, \theta)$ the time derivative of the energy of particles trapped in the wave is either positive or negative in all points of the exact resonance $\omega = |\omega_t|$, except for X-points and O-points of the resonance islands.

Because GAMs do not change the particle magnetic moment and $\omega_t = v_\parallel/(qR)$, $\omega_E = -c\hat{E}/(\kappa_e r \bar{B})$ [q is the safety factor, R is the distance from the major axis of the torus, $\bar{B} = B(r = 0)$], equation (4) can be written as

$$\langle \dot{r} \rangle = \frac{qR_s}{\omega_B \kappa_e r} \langle \dot{v}_\parallel \rangle, \tag{6}$$

where ω_B is the gyrofrequency, R_s is the radius of the magnetic axis. Noting that $\langle v_\parallel \rangle \approx v_\parallel(\theta = \pi/2) \equiv u$ and neglecting the magnetic shear, we obtain from (6):

$$\Delta(r^2) = \frac{2qR_s}{\omega_B \kappa_e} \Delta u. \tag{7}$$

This agrees with the more general relation

$$MR_s \Delta u = \frac{e}{c} \Delta\psi_P(\pi/2) \tag{8}$$

(ψ_P is the poloidal magnetic flux on the particle orbit, $\psi_P(\pi/2) \equiv \psi_P[r(\theta = \pi/2)]$), which immediately follows from the conservation of the canonical angular momentum, $P_\phi = Mv_\parallel R - e\psi_P/c = \text{const}$.

Note that, as seen from (7), the particle displacement due to the GAM-induced slowing down cannot exceed its poloidal Larmor radius. Thus, this effect can be considerable only in current experiments but not in ITER-size machines.

In order to demonstrate the change of the energy and location of the passing resonant ions driving a GAM / E-GAM instability, we solved numerically the following equations:

$$\frac{dx}{d\tau} = -\frac{1+\chi^2}{1+\chi_0^2} \bar{\omega}_D W \sin\theta, \tag{9}$$

$$\frac{d\theta}{d\tau} = \frac{\chi}{\chi_0}\sqrt{W} - \bar{\omega}_D \frac{W}{x} \frac{1+\chi^2}{1+\chi_0{}^2} \cos\theta - \frac{\bar{\omega}_E}{x} \sin(\theta - \theta_0), \tag{10}$$

$$\frac{dW}{d\tau} = -\frac{1+\chi^2}{1+\chi_0^2} \bar{\omega}_D W \sin\theta \sin(\theta - \theta_0), \tag{11}$$

where $x = r/a$, a is the plasma radius in the equatorial plane of the torus, $\tau = t\omega_{t0}$, $W = \mathcal{E}/\mathcal{E}_0$, the subscript '0' labels magnitudes at $t = 0$, $\chi = \sigma\sqrt{1 - W_\perp/W}$ is the particle pitch angle cosine, $W_\perp = \mathcal{E}_\perp/\mathcal{E}_0$, $\mathcal{E}_\perp = \text{const}$ is the transverse energy, $\bar{\omega}_D = \omega_{Da}/\omega_{t0}$, $\bar{\omega}_E = \omega_{Ea}/\omega_{t0}$, $\omega_{Ea} = c\hat{E}/(a\bar{B}\kappa_e)$, $\omega_{Da} = v_{D0}/(a\kappa_e) = 0.5(1 + \chi_0^2)\rho_0 v_0/(R_s a \kappa_e)$, $\rho = v/\omega_B$ is the Larmor radius.

Equations (9)–(11) are actually equations (1) written in the assumption that the fast ion remains resonant in spite of the fact that its longitudinal energy and the radial location change. This can be the case when the width of the resonance in the phase space and the radial mode width are large enough (strictly speaking, when the resonant region is infinite). In reality, the mode width depends on the fast ion orbit width [7] and the magnitude of β [10].

The results of calculation for a deuteron with $\mathcal{E} = 75$ keV, $\chi_0 = 0.7$, and DIII-D parameters [6] ($R_s = 170$ cm, $a = 60$ cm, $\kappa_e = 1.3$, $T = 1.5$ keV, and $q = 4$) are shown in figure 1. The GAM amplitude was taken from the equation $\hat{E}_r = \text{const} = \Phi/L = 5\ \text{kV m}^{-1}$, with $e\Phi = T$ and $L = 0.3$ m, which seems realistic (the local E_r can be much higher, up to 28 keV m^{-1}) [8]. Figure 1 confirms our consideration above. In addition, it shows that a considerable effect of the mode takes place for a few tens of the transits ($\tau = 200$ corresponds to 32 transits—about 1 ms), which is much less than the collisional slowing down time and the duration of the instability bursts (several ms) in the experiment. However, we should note that equations (9)–(11) describe the motion of well-passing ions, whereas mainly marginally passing ions with $\mathcal{E} = 75$ keV were resonant in DIII-D experiments, see section 3.2. This means that more complicated equations should be used to describe the motion of energetic ions during E-GAM in DIII-D.

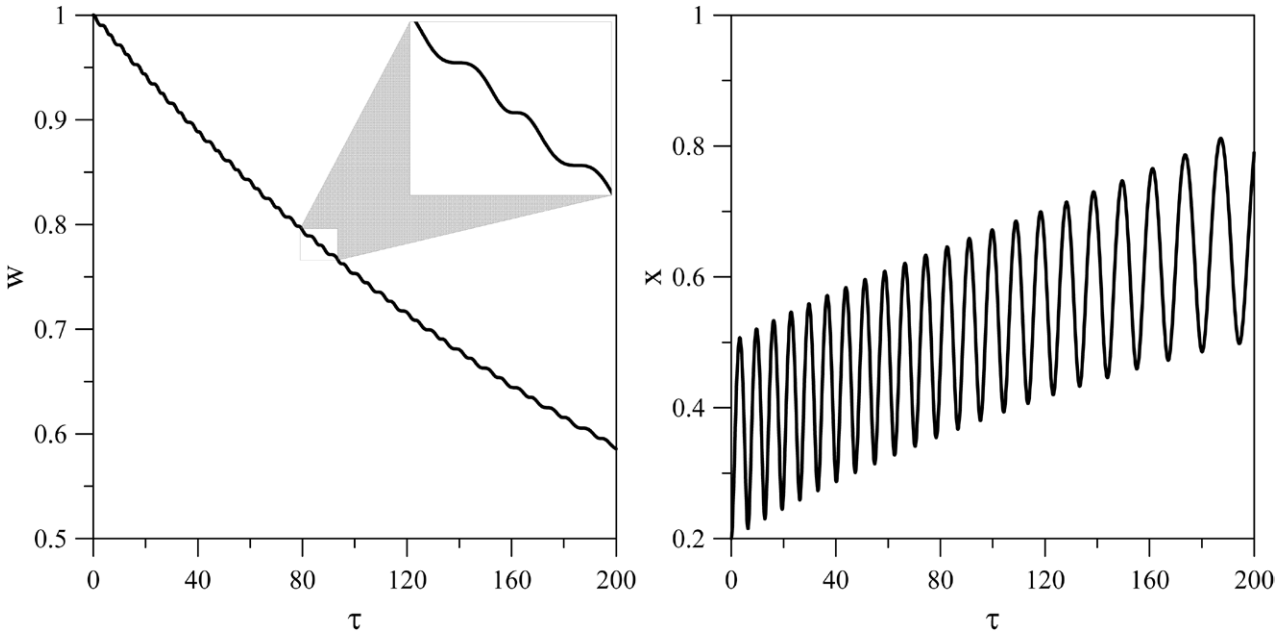

Figure 1. Normalized energy, W, and radial coordinate, x, versus $\tau \equiv t\omega_{t0}$ ($\omega_{t0} = \omega_t(t=0)$) of the fast ions driving the instability. Calculations are carried out in the assumptions that the ions are well passing and the resonance condition $\omega = |\omega_t|$ is satisfied during the evolution.

Finite width of the resonance region leads to an oscillation of the transit-time averaged orbit of the particle in the phase space, i.e. leads to bounce motion inside the island ('superbanana motion'). A rigorous theory giving both the oscillation frequency and the resonance width as functions of characteristics of the mode and the plasma is developed in appendix A. Below we obtain these results by means of a simple but less rigorous procedure.

First of all, we note that in the vicinity of the resonance, i.e. when $|\omega_t - \omega| \ll \omega$, equation (5) approximately holds: $J \approx 0.5\cos(\theta_0 + \pi(1 - \omega/\omega_t))$. Therefore, θ_0 determines $\langle\dot{\mathcal{E}}\rangle$ during the particle motion along a superbanana orbit in the $(\mathcal{E}, \theta_0)$ space. In other words, θ_0 plays the role of a slow coordinate governed by

$$\ddot{\theta}_0 = \langle\dot{\omega}_t\rangle = \frac{\langle\dot{v}_\parallel\rangle}{qR_s} - \frac{\hat{s}v_\parallel}{qR_s}\frac{\langle\dot{r}\rangle}{r}, \tag{12}$$

($\hat{s}$ is the magnetic shear), which follows from the equation $\dot{\theta} = \omega_t$. Here $\langle\dot{r}\rangle$ can be eliminated due to relation (6). As a result, we have:

$$\ddot{\theta}_0 = \frac{\langle\dot{v}_\parallel\rangle}{qR_s}\Xi, \tag{13}$$

where

$$\Xi = 1 - \frac{\hat{s}q\rho_\parallel}{\kappa_e r\epsilon}, \tag{14}$$

and $\rho_\parallel = v_\parallel/\omega_B$, $\epsilon = r/R_s$. Here averaged values vary in time due to the presence of the GAM mode. To calculate $\langle\dot{v}_\parallel\rangle$, we use equation (3) and assume that the transverse energy is conserved (due to the conservation of the magnetic moment). Then

$$\langle\dot{v}_\parallel\rangle = -\frac{e\hat{E}}{2M\kappa_e}\frac{v_D}{v_\parallel}\cos\theta_0. \tag{15}$$

Combining equations (13) and (15) we obtain a well-known pendulum equation:

$$\ddot{\vartheta} + \omega_{isl}^2\sin\vartheta = 0, \tag{16}$$

where $\vartheta = \theta_0 - \pi/2$ and

$$\omega_{isl} = \left|\frac{e\hat{E}}{2M}\frac{v_D}{v_\parallel^2}\omega\frac{\Xi}{\kappa_e}\right|^{1/2}. \tag{17}$$

The frequency ω_{isl} represents the frequency of the particle bounce motion inside the island. Note that the negative magnetic shear increases ω_{isl}, whereas the positive one decreases it, unless the magnetic shear is so large that the second term in (14) exceeds unity.

Now we can evaluate the island width, i.e. the width of the resonant region, as $\sim \langle\dot{v}_\parallel\rangle\tau_{isl}$, where $\tau_{isl} = 2\pi/\omega_{isl}$ and $\langle\dot{v}_\parallel\rangle$ is given by equation (15). This agrees with the rigorous consideration in appendix A (see also [12]), where it was found that

$$|\Delta u^{res}| = 4\left|\frac{e}{M\omega\Xi}\overline{\boldsymbol{v}_D\cdot\tilde{\boldsymbol{E}}}\right|^{1/2} \approx 2\sqrt{2}\left|\frac{e}{M\omega\kappa_e\Xi}v_D\hat{E}\right|^{1/2}, \tag{18}$$

where the line above letters denotes time averaging, $v_D = \rho v(1+\chi^2)/(2R_s)$.

It follows from equation (18) that in the energy space the resonance width depends on χ linearly, $\Delta\mathcal{E}^{res} \propto \chi$. This indicates that $\Delta\mathcal{E}^{res}$ for marginally passing particles is minimum (see also sections 3.2 and appendix A).

Comparing equation (17) with equation (18), we find:

$$\frac{\omega_{\rm isl}}{\omega} = \frac{\Xi}{4}\frac{\Delta u^{\rm res}}{u^i}. \tag{19}$$

The same relation can be obtained directly from equation (16). It follows from this equation that the island width in the plane $(\theta, \dot\theta)$ is $\Delta\dot\theta = 4\omega_{\rm isl}$. Taking $\dot\theta = \omega_t = v_\parallel/(qR)$ and using the resonance condition $|\omega_t| = \omega$, we immediately arrive at equation (19).

From equation (18) we have:

$$\left|\frac{\Delta u^{\rm res}}{u^i}\right| = 2\left|\frac{(2-\lambda^i)|\hat v_E|}{(1-\lambda^i)\omega\kappa_e R_s \Xi}\right|^{1/2}, \tag{20}$$

where $v_E = c\hat E/\bar B$, $\lambda = \mu_p \bar B/\mathcal{E}$, μ_p is the particle magnetic moment, the superscript i labels magnitudes before the GAM mode appears. Because experimentally measured magnitude is the amplitude of the electron density fluctuation, $\hat n$, let us express $\hat E_r$ through $\hat n$. This can be done by proceeding from ideal MHD equations (e.g. those derived in [13]), which couple the electric potential and plasma compressibility through the field line curvature. As a result, we obtain (see [11]):

$$\left|\frac{\Delta u^{\rm res}}{u^i}\right| = 2\left|\frac{\mathcal{S}}{\Xi}\,\frac{2-\lambda^i}{1-\lambda^i}\,\frac{\hat n}{n_0}\right|^{1/2}, \tag{21}$$

where $\mathcal{S} = 1 - k_s^2 c_s^2/\omega^2$, $\Delta u^{\rm res}/u^i < 0$ for the slowing down and $\Delta u^{\rm res}/u^i > 0$ for the acceleration.

Following [11], we assume that $\mathcal{E}^f = \mathcal{E}^i + \Delta\mathcal{E}^{\rm res}$, where $\Delta\mathcal{E}^{\rm res}$ is the energy resonance width, $\Delta\mathcal{E}^{\rm res}/\mathcal{E}^i = (1-\lambda^i)(2+\Delta u^{\rm res}/u^i)\Delta u^{\rm res}/u^i$, the superscript f labels magnitudes after interaction with the mode. Due to this assumption, we will obtain the maximum possible cooling of an energetic ion because it implies that the ion moves across the whole resonance region. Then, using equation (21) with $\Delta u^{\rm res}/u^i < 0$ (which is true when the energy decreases), we obtain:

$$\frac{\mathcal{E}^f}{\mathcal{E}^i} = 1 - 4\sqrt{2\mathcal{S}\frac{\hat n}{n_0}}\left(\sqrt{1-\lambda^i} - \sqrt{2\mathcal{S}\frac{\hat n}{n_0}}\right). \tag{22}$$

Note that $|\Delta u^{\rm res}|/|u^i| \leqslant 1$ in the case of slowing down, from which it follows that equation (22) is valid for

$$\sqrt{1-\lambda^i} > 2\left(2\mathcal{S}\frac{\hat n}{n_0}\right)^{1/2}. \tag{23}$$

For instance, $\mathcal{E}^f/\mathcal{E}^i = 0.6$–$0.7$ for $\lambda = 0$–0.3, $\mathcal{S} = 1$ and $\hat n/n_0 = 1\%$. We conclude from here that the resonant interaction of the well-passing energetic ions and a global GAM / E-GAM mode can lead to the transfer of a large fraction of the energy of these ions to the mode, which is accompanied by radial displacements of the particles.

3. Drops of the neutron emission

3.1. General relations

In this section we consider a possible change of the neutron emission during bursts of the GAM / E-GAM instability. We assume that neutrons are produced mainly due to beam-plasma fusion reactions and that the instability affects only the beam, but not the plasma. Our other assumptions are that there is no orbit transformation under the influence of the mode and that the number of fast ions is conserved, which corresponds to our analysis above.

In this section we derive and analyse general relations for the change of fusion reactivity in the case when the fast ion population consists of well-passing particles. In section 3.2 the obtained relations will be generalized to be valid for the marginally passing particles in connection with the DIII-D experiment [6].

Let us proceed from a general relation for the beam-plasma fusion reaction rate, I, given by

$$I = \int {\rm d}^3x\, I_{\rm L}, \tag{24}$$

where the integral is taken over the plasma volume, and $I_{\rm L}$ is the local reaction rate,

$$I_{\rm L} = \int {\rm d}^3v\, {\rm d}^3v'\, F_p(\boldsymbol{r}', \boldsymbol{v}')F_b(\boldsymbol{r}, \boldsymbol{v})\sigma|\boldsymbol{v} - \boldsymbol{v}'|, \tag{25}$$

where $\sigma \equiv \sigma(|\boldsymbol{v} - \boldsymbol{v}'|)$ is the cross section of a fusion reaction, $F_p(\boldsymbol{r}, \boldsymbol{v})$ and $F_b(\boldsymbol{r}, \boldsymbol{v})$ are the distribution function of plasma ions and the distribution function of beam ions, respectively. Assuming that the particle orbit width is small and taking into account that the beam ion velocity well exceeds the thermal velocity of the plasma ions, we can write $F_p = n_p(r)\delta(\boldsymbol{v})$ and $F_b = n_b(r)f_b(\boldsymbol{v})$, where n_p and n_b are the particle density, the subscripts p and b refer to plasma and beam quantities, respectively, $\delta(x)$ is the Dirac delta function. Then we can approximate equation (25) as [14]

$$I_{\rm L} = n_p n_b \langle\sigma v\rangle_b, \tag{26}$$

where $\langle\sigma v\rangle_b = \int {\rm d}^3v f_b(\boldsymbol{v})\sigma(v)v$.

Note that assuming $F_p = n_p(r)\delta(\boldsymbol{v})$ to obtain (26), we actually took the plasma temperature $T = 0$ and neglected the plasma rotation. The validity of these assumptions is discussed in appendix C, where it is shown that effects of the plasma temperature and plasma rotation on the fusion reaction rate tend to compensate each other when the direction of the plasma rotation coincides with the beam direction.

Using equations (24) and (26) and the fact that $\langle\sigma v\rangle^i$ does not depend on the spatial coordinates, we obtain the following expression for the change of the fusion reaction rate because of the instability:

$$\frac{\Delta I}{I^i} = \frac{\int_{\psi_1}^{\psi_2} {\rm d}\psi\, n_p(n_b^f\xi - n_b^i)}{\int_0^1 {\rm d}\psi\, n_p n_b^i}, \tag{27}$$

where $\xi = \langle\sigma v\rangle_b^f/\langle\sigma v\rangle_b^i$, $\psi = r^2/a^2$, ψ_1 and ψ_2 are characteristic boundaries of the mode location.

It is clear that in the case of D–D reaction, equation (27) describes the change of the neutron emission correctly provided that σ is selected for that channel of the reaction which is associated with the neutron production.

The change of the neutron yield is maximum when the resonant interaction involves ions with the highest energy, $\mathcal{E} \sim \mathcal{E}_\alpha$, where $\mathcal{E}_\alpha$ is the birth energy of fast ions. Both a distortion of

the velocity distribution of these ions and their radial redistribution contribute to the change of the neutron emission. It is not clear *a priori* whether both factors are important. To clarify it, let us analyse equation (27).

Assuming first that the plasma is homogeneous and using the conservation of the particle number we can write:

$$\frac{\Delta I}{I^i} = (\xi - 1)\frac{\delta N_b}{N_b}, \tag{28}$$

where N_b and δN_b are the total number of fast ions and the number of these ions in the region of the mode location, respectively. It follows from (28) that the radial redistribution of fast ions (without their loss) in homogeneous plasmas does not change the neutron yield, $\Delta I = 0$, when $\xi = 1$, i.e. when the GAM influence on the velocity distribution of energetic ions is negligible. This is not surprising. However, in reality $f(\boldsymbol{v})$ can be strongly affected by the instability, so that a plateau in the resonance region is formed. This will be the case when

$$\tau_{\rm isl} \ll (\Delta t)_{\rm ins} \ll \tau_{\rm col}, \tag{29}$$

where $\tau_{\rm isl} = 2\pi/\omega_{\rm isl}$, $(\Delta t)_{\rm ins}$ is the duration of the instability burst, $\tau_{\rm col}$ is a characteristic collisional time (for instance, the slowing down time). Equation (28) predicts the largest drops of the neutron yield for $\xi \ll 1$, leading to

$$\frac{\Delta I}{I^i} \approx -\frac{\delta N_b}{N_b}. \tag{30}$$

This ratio is rather large provided that the mode occupies a considerable part of the plasma cross section.

In order to see the role of plasma inhomogeneity, let us eliminate the influence of the velocity distortion of the fast ion distribution by taking $\xi = 1$. Then, assuming that the plasma density in the region of the mode location can be approximated as $n_p = n_{p1} + n'_{p1}(\psi - \psi_1)$, with $n'_{p1} = {\rm d}n_p/{\rm d}\psi|_{\psi_1}$, we obtain:

$$\frac{\Delta I}{I^i} = -\frac{n'_{p1}\int_{\psi_1}^{\psi_2} {\rm d}\psi\, \psi(n_b^i - n_b^f)}{\int_0^1 {\rm d}\psi\, n_p n_b^i}. \tag{31}$$

The integral in the numerator does not vanish due to the presence of the factor ψ under the integral. It can be written as $\int_{\psi_1}^{\psi_2} {\rm d}\psi\, \psi(n_b^i - n_b^f) \sim \alpha\psi_1\delta n_b\Delta\psi$, where $\alpha < 1, \Delta\psi = \psi_2 - \psi_1$, δn_b is a characteristic magnitude of the change of the beam density due to the GAM mode. Thus, equation (31) reads:

$$\frac{\Delta I}{I^i} = \alpha\Delta\psi\frac{|\delta n_b|}{n_b}\frac{{\rm d}\ln n_p}{{\rm d}\psi}\bigg|_{\psi_1}. \tag{32}$$

This equation predicts $|\Delta I|/I^i \ll 1$, $\Delta I < 0$ when $n_p(r)$ is a decreasing function in the region where the mode is located.

It follows from (28) and (32) that the velocity distortion may be mainly responsible for the change of the neutron yield when $\xi \ll 1$.

In order to see whether ξ can be small, below we derive an expression for ξ assuming, first, that a GAM / E-GAM instability arises shortly after switching on the Neutron Beam Injection (NBI) and, second, that energetic ions with the birth energy are resonant. In this case we can take $f_b(\boldsymbol{v}) = f_\parallel(v_\parallel)f_\perp(\boldsymbol{v}_\perp)$, with $\int {\rm d}v_\parallel f_\parallel = 1$ and $\int {\rm d}\boldsymbol{v}_\perp f_\perp = 1$ and $f_\parallel^{(i)} = \delta(v_\parallel - v_{\parallel\alpha})$, $f_\perp^{(i)} = f_\perp^{(f)} = \delta(\boldsymbol{v}_\perp - \boldsymbol{v}_{\perp\alpha})$. To evaluate a maximum possible effect of the influence of a GAM /E-GAM, we assume that all the resonant particles slow down due to the instability, leading to $f_\parallel^{(f)} = {\rm const}$ in the region $v_{\parallel 1} \leqslant v_\parallel \leqslant v_{\parallel\alpha}$. Then, taking into account that GAMs conserve the particle magnetic moment, we have:

$$\langle\sigma v\rangle_b^{(i)} = \sigma(v_\alpha)v_\alpha, \quad \langle\sigma v\rangle_b^{(f)} = f_\parallel^{(f)}\int_{v_{\parallel 1}}^{v_{\parallel\alpha}} {\rm d}v_\parallel\, \sigma\left(\sqrt{v_\parallel^2 + v_{\perp\alpha}^2}\right)\sqrt{v_\parallel^2 + v_{\perp\alpha}^2}, \tag{33}$$

where $f_\parallel^{(f)}$, as follows from the conservation of the number of particles, is given by

$$f_\parallel^{(f)} = \frac{1}{v_{\parallel\alpha} - v_{\parallel 1}}. \tag{34}$$

By means of equations (33) and (34), one can write the following relation convenient for the calculation of ξ:

$$\xi = \frac{1}{2\sigma(\mathcal{E}_\alpha)}\frac{v_\alpha}{\Delta v_\parallel^{\rm res}}\int_{W_{\rm min}}^1 {\rm d}W\, \sigma(W\mathcal{E}_\alpha)\sqrt{\frac{W}{W - 1 + \chi_\alpha^2}}, \tag{35}$$

where $W = \mathcal{E}/\mathcal{E}_\alpha$, $\Delta v_\parallel^{\rm res} = v_{\parallel\alpha} - v_{\parallel 1}$, $\chi_\alpha = v_{\parallel\alpha}/v_\alpha$.

$$W_{\rm min} = 1 - \chi_\alpha^2 + \left(\chi_\alpha - \frac{\Delta v_\parallel^{\rm res}}{v_\alpha}\right)^2. \tag{36}$$

At the injection energy $\mathcal{E}_\alpha < 100$ keV, the cross section of the D–D reaction strongly depends on the particle energy. In this case a region close to $W = 1$ mainly contributes to the integral in (35); therefore, we can write $\xi = (\Delta v_\parallel)^{\rm ef}/\Delta v_\parallel^{\rm res} < 1$,

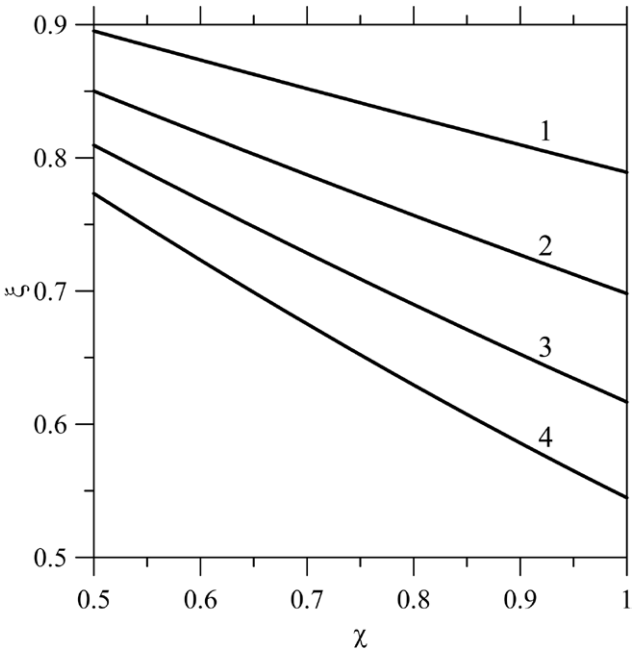

Figure 2. ξ versus χ according to equation (35). The calculations were carried out for different magnitudes of the ratio $\Delta v_\parallel^{\rm res}/v_\alpha$: 1, 0.1; 2, 0.15; 3, 0.2; 4, 0.25.

Table 1. The characteristic times in the DIII-D experiments described in [6].

τ_t	$\tau_{\rm isl}$	GAM burst duration	Time between NBI start and 1st GAM burst	GAM activity duration	τ_s
0.04 ms	0.64 ms	1.5–2 ms	8 ms (weak burst), 15 ms (strong burst)	⩽30 ms	540 ms

Note: It was assumed that $f = 25$ kHz, $q = 4$, $\Delta v_\parallel^{\rm res}/v_\parallel = 1/4$, $T = 1.8$ keV, $n_{\rm e} = 10^{13}$ cm^{-3}. The estimates of τ_t and $\tau_{\rm isl}$ are made for well-passing particles, $\tau_t = 2\pi/|\omega_t|$ with $|\omega_t| = \omega$, $\tau_{\rm isl} = (4/f)(v_\parallel/\Delta v_\parallel^{\rm res})$, τ_s is the collisional slowing-down time.

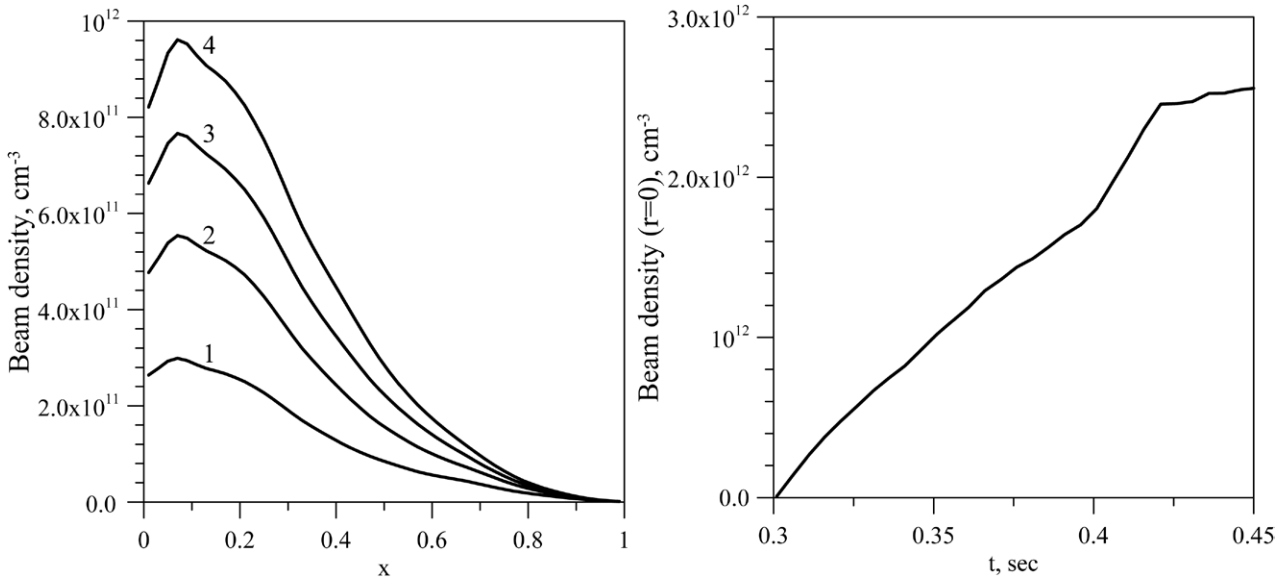

Figure 3. Temporal evolution of energetic ion density in DIII-D. Left panel, $n_b\,(x)$ with $x = r/a$ in various moments of times (1, $t_1 = 0.311$ s; 2, $t_2 = 0.321$ s; 3, $t_3 = 0.331$ s; 4, $t_4 = 0.341$ s); right panel, $n_b(r = 0)$ versus time. We observe that the radial profile of n_b weakly changes, whereas the central density approximately linearly grows till $t_* \sim 0.4$ s. This indicates that the number of energetic particles approximately linearly grows till t_*.

where $(\Delta v_\parallel)^{\rm ef} = v_{\parallel\alpha} - v_\parallel^{\rm ef}$, $v_\parallel^{\rm ef}$ is a characteristic minimum longitudinal velocity of energetic ions responsible for the neutron emission. The ratio $(\Delta v_\parallel)^{\rm ef}/\Delta v_\parallel^{\rm res}$ and, thus, ξ, decreases when $\Delta v_\parallel^{\rm res}$ grows. Numerical calculations confirm this, see figure 2. We infer from this figure and equation (28) that the distortion of the velocity distribution of the energetic ions can considerably affect drops of the neutron emission when the resonance region is sufficiently wide.

Note that the energies of the resonant particles can be much less than the birth energy. In this case the influence of the GAM mode on the neutron emission will be less than our estimate made.

3.2. E-GAM experiment on DIII-D

Let us consider a possible influence of the E-GAM induced distortion of $F_b(\boldsymbol{r}, \boldsymbol{v})$ on drops of the neutron emission in the DIII-D experiment described in [6].

The E-GAM instability had a bursting character, each burst lasted for 1.5–2 ms (see figure 1 of [6]). Therefore, a question arises whether this time was sufficient for the mode to produce a plateau in the resonance region of the velocity space. In other words, we need to know whether the conditions (29) are satisfied. This and other relevant information can be got from the comparison of characteristic times shown in table 1. Note that the estimates of τ_t and $\tau_{\rm isl}$ are made for well-passing particles.

First of all, we draw attention to the fact that the E-GAM activity started in $(\Delta t)_1 \sim 10$ ms after the beginning of NBI and lasted for about $(\Delta t)_2 = 30$ ms, the phase of strong neutron drops was lasting only for 20 ms. On the other hand, the collisional slowing down time was more than 500 ms, which by a factor of 10 exceeds $(\Delta t)_1 + (\Delta t)_2$. Thus, the GAM activity stopped well before the well-known collisional distribution of energetic ions, $F_b \propto 1/v^3$, in a wide velocity range was formed. This implies that the energetic ions had predominantly the birth pitch-angles and energy during E-GAM activity.

A numerical calculation of temporal evolution of the distribution function of α-particles shows that when $\Delta t/\tau_s \leqslant 0.1$, the effect of Coulomb collisions on the shape of $f_\alpha(v)$ is really small (see figure 8 in [15]). Figure 3 also supports our conclusion. It shows that in DIII-D the number of energetic ions quickly grows approximately linearly till $t_* \sim 400$ ms, whereas it should be nearly constant if the collisional distribution has been formed.

Figure 3 was obtained as explained below.

Equilibrium reconstruction was performed from within the OMFIT [16] workflow manager using EFIT [17] with constraints from magnetics, motional stark-effect (MSE) internal pitch-angle measurements, thermal pressure from Thomson scattering and charge-exchange recombination

(CER) spectroscopy, and total pressure including neutral beam injected ions computed by TRANSP [18] with NUBEAM Monte-Carlo package [19]. Due the presence of fast-ion instabilities, an *ad hoc* anomalous fast-ion diffusion was employed for the equilibrium reconstruction to recover the experimental neutron rate and total stored energy. A reconstruction with MSE as the sole internal measurement results in a non-physical negative central pressure, and this procedure adds the missing pressure information to obtain a valid reconstruction. The refined equilibrium reconstruction was then used in TRANSP with NUBEAM a final time to produce the final fast-ion distribution function used in this work.

To proceed further, we have to analyze the resonance condition. For the passing particles it can be written as follows:

$$\omega = \frac{\pi}{2\mathbf{K}(\kappa_p^{-1})}\frac{|\hat{v}_\parallel|}{qR}, \tag{37}$$

where $\mathbf{K}(\kappa_p^{-1})$ is the elliptic integral of the first kind, κ_p is the particle trapping parameter defined by $\kappa_p^{-2} = 2\epsilon\hat{v}_\perp^2/\hat{v}_\parallel^2$, $\hat{v}_\parallel \equiv v_\parallel(\theta = 0)$, $\hat{v}_\perp \equiv v_\perp(\theta = \pi/2)$, $\lambda = \hat{\mathcal{E}}_\perp/\mathcal{E}$, $\hat{\mathcal{E}}_\perp = M\hat{v}_\perp^2/2$ [20].

For a deuteron with the birth velocity $v_\alpha = 2.7 \times 10^8$ cm s^{-1} (the birth energy $\mathcal{E}_\alpha = 75$ keV), the mode frequency $f = 25$ kHz, and major radius of the torus $R_s = 170$ cm equation (37) is reduced to

$$\frac{\pi|\hat{\chi}_\alpha|}{2\mathbf{K}(y_\alpha)} = 0.1q(r), \tag{38}$$

where

$$y_\alpha \equiv y(\hat{\chi} = \hat{\chi}_\alpha), \quad y(\hat{\chi}) = \left(\frac{2\epsilon}{1-\epsilon}\frac{1-\hat{\chi}_\alpha^2}{\hat{\chi}^2}\right)^{1/2}, \tag{39}$$

$\hat{\chi} = \hat{v}_\parallel/v_\alpha$, $\hat{\chi}_\alpha = \hat{v}_\parallel(v_\alpha)/v_\alpha$. This equation determines $\hat{\chi}_\alpha$ (and other pitch-angle parameters) as a function of r when the exact resonance condition is satisfied. Numerical solution of (38) with $q(r)$ given by figure 2 of [6] shows that well-passing resonant ions ($\kappa_p^2 \gg 1$) can exist only in the near-axis region and near the plasma edge; in the region of the mode location ($0.2 < r/a < 0.5$) resonant particles are marginally passing and characterized by $\kappa_p^2 < 2$, see figure 4.

Therefore, we have to generalize relations obtained in previous sections in order to describe the experiment correctly.

Equation for the frequency of the drift motion inside the island at $\kappa_p \gtrsim 1$ can be derived by means of the same procedure as in section 2, but with the resonance given by equation (37). The matter is that the basic equations (3) and (5) are valid not only for the well passing particles but also for almost all marginally passing particles, see figure A1. Neglecting for simplicity effects of the magnetic shear (described by the factor Ξ in (37)) we obtain:

$$\omega_{\rm isl} = \left(\frac{\mathbf{E}(\kappa_p^{-1})}{\mathbf{K}(\kappa_p^{-1})}\frac{e\hat{E}}{2M\kappa_{\rm e}}\frac{v_{\rm D}}{v_\parallel^2(\pi)}\omega\right)^{1/2}, \tag{40}$$

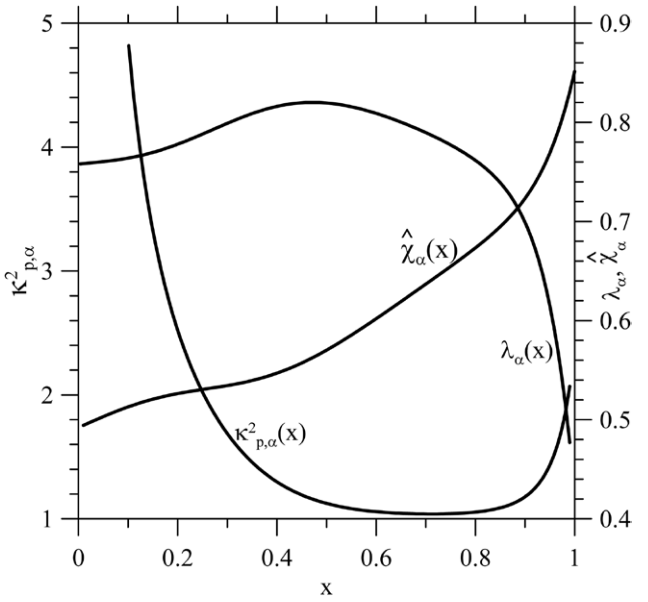

Figure 4. The pitch-angle parameters $\kappa_{p,\alpha}$, λ_α, and $\hat{\chi}_\alpha$ versus $x \equiv r/a$ of a passing resonant 75 keV deuteron in DIII-D, which are determined by equation (38). It follows from this figure that most of the resonant particles with high energy (75 keV) are marginally passing. The well passing resonant particles can exist only at $x < 0.2$ and near the plasma edge.

where $v_\parallel(\pi) \equiv v_\parallel(\theta = \pi) = \hat{v}_\parallel\sqrt{1-\kappa_p^{-2}}$. It follows from (40) that $\omega_{\rm isl}$ is a growing function of κ_p^{-1} (it grows very weakly, unless $\kappa_p \to 1$).

We infer from here that the plateau in the velocity distribution of the marginally passing energetic ions is formed even faster than in the case of the well passing ones. Therefore, the conclusion that the period of the island bounce motion is less than the duration of E-GAM bursts in DIII-D, which follows from table 1, remains valid for marginally passing particles. This implies that parameters of the E-GAM can be treated as time independent in spite of the bursting character of the instability in DIII-D.

On the other hand, the island width, i.e. the resonance width, of marginally passing particles is less than that of the well passing ones. It is given by (see appendix A):

$$\Delta\mathcal{E}^{\rm res} = 4v_\parallel(\pi)\left(\frac{\mathbf{K}(\kappa_p^{-1})}{\mathbf{E}(\kappa_p^{-1})}\frac{eMv_{\rm D}\hat{E}_r}{2\omega\kappa_{\rm e}}\right)^{1/2}. \tag{41}$$

This can be written in terms of longitudinal velocity as (see equation (18)):

$$\Delta\hat{v}_\parallel^{\rm res} \approx 2\sqrt{2}\left[(1-\kappa_p^{-2})\frac{\mathbf{K}(\kappa_p^{-1})}{\mathbf{E}(\kappa_p^{-1})}\frac{ev_{\rm D}\hat{E}_r}{M\omega\kappa_{\rm e}}\right]^{1/2}. \tag{42}$$

The decrease of the resonance width and the increase of the bounce island frequency of marginally passing particles is described by the factor $\Theta \equiv \tau_{\rm isl}^0/\tau_{\rm isl} \sim \sqrt{\mathbf{E}(\kappa_p)/\mathbf{K}(\kappa_p)}\, v_\parallel^0/v_\parallel(\pi) = \sqrt{(\mathbf{E}(\kappa_p)/\mathbf{K}(\kappa_p))}/\sqrt{(1-\kappa_p^{-2})}$, where the superscript '0' labels particles with $\kappa_p^2 \gg 1$. For

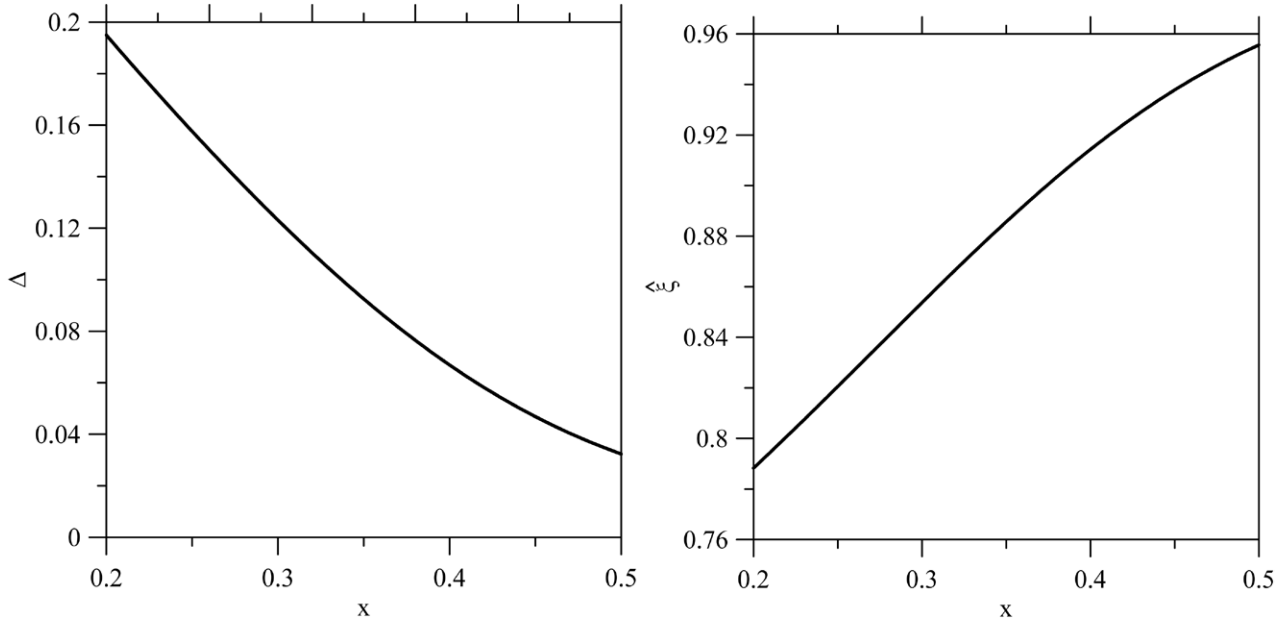

Figure 5. The resonance width, $\Delta \equiv \Delta\hat{v}_\parallel^{\rm res}/v_\alpha$, and the mode-induced change of the fusion reaction rate, $\hat{\xi} \equiv \langle\sigma v\rangle^f/\langle\sigma v\rangle^i$, versus $x = r/a$ in the region of E-GAM location in DIII-D. The function $\Delta(x)$ is strongly decreasing because the separatrix $\kappa_p^2 = 1$ cuts the resonance region of marginally passing particles. This also explains why $\hat{\xi}(x)$ is a growing function.

instance, taking $\kappa_p = 1.1$, we obtain $\Theta = 1.009$ (although $\Theta = \infty$ for $\kappa_p = 1$). This means that in many cases relations for the bounce island frequency and the islands width obtained in section 2 for well passing particles remain valid for marginally passing particles. In particular, the following relation for the resonance width is true unless $(\kappa_p - 1) \ll 0.1$:

$$\frac{\Delta\mathcal{E}^{\rm res}}{\mathcal{E}} \approx 4\frac{\hat{v}_\parallel}{v}\left[\mathcal{S}\frac{\hat{n}_{\rm e}}{n_0}\left(1 + \frac{\hat{v}_\parallel^2}{v^2}\right)\right]^{1/2}. \qquad (43)$$

Let us obtain now equations describing the change of the neutron emission when a population of the energetic ions contains marginally passing particles.

First of all, we note that the following equation is valid for the passing particles:

$$\int \mathrm{d}^3x \int \mathrm{d}^3v\, G = \frac{4\pi^2 c}{eM^2}\sum_{\sigma_v}\int \mathrm{d}P_\phi\, \mathrm{d}\mathcal{E}\, \mathrm{d}\mu_p\, \tau_t G, \qquad (44)$$

where G is an arbitrary function of the constants of motion (P_ϕ, $\mathcal{E}$, μ_p, and σ_v). Due to this relation, we can write:

$$\frac{\Delta I}{I^i} = \frac{\int \mathrm{d}\psi\, n_p \int \mathrm{d}\hat{v}_\parallel \int \mathrm{d}\hat{v}_\perp\, \hat{v}_\perp \mathbf{K}(\kappa_p^{-1})\sigma(v)v(F_b^f - F_b^i)}{\int \mathrm{d}\psi\, n_p \int \mathrm{d}\hat{v}_\parallel \int \mathrm{d}\hat{v}_\perp\, \hat{v}_\perp \mathbf{K}(\kappa_p^{-1})\sigma(v)vF_b^i}, \qquad (45)$$

Taking $F_b \propto n_b\delta(\hat{v}_\parallel - v_{\parallel\alpha})\delta(\hat{v}_\perp - v_{\perp\alpha})$, we obtain equation (27), where, however, ξ is not determined by (35) but should be replaced by

$$\hat{\xi} = \frac{\int_{\hat{\chi}_\alpha - \Delta}^{\hat{\chi}_\alpha} \mathrm{d}\hat{\chi}\, \Lambda\sigma(v)v}{\sigma(v_\alpha)v_\alpha \int_{\hat{\chi}_\alpha - \Delta}^{\hat{\chi}_\alpha} \mathrm{d}\hat{\chi}\, \Lambda}, \qquad (46)$$

where $\Lambda = \mathbf{K}(y)/\mathbf{K}(y_\alpha)$, $v = v_\alpha\sqrt{1 + \hat{\chi}^2 - \hat{\chi}_\alpha^2}$; $\Delta = \Delta\hat{v}_\parallel^{\rm res}/v_\alpha$, unless $\hat{\chi} = \hat{\chi}_\alpha - \Delta$ corresponds to $\kappa_p^2 < 1$, in which case Δ is restricted by the condition $\kappa_p^2 > 1$.

Using equation (46) and DIII-D parameters, we calculated Δ and then $\hat{\xi}(x)$ shown in figure 5. We observe that Δ strongly varies within the mode location ($0.2 < x < 0.5$), changing by a factor of 5. This indicates that many particles can reach a vicinity of the separatrix, see figure 6. Some of them, which were born close to the separatrix, reach it for the time $\Delta t \ll \tau_{\rm isl}$. These particles either undergo the orbit transformation (becoming toroidally trapped) or they are reflected from the separatrix region and gain the energy. Maybe, both processes take place. Our theory is not sufficient to predict their behaviour. The described dependence of Δ on x explains why $\hat{\xi}(x)$ (which represents the change of $\langle\sigma v\rangle$ due to the instability) is a growing function.

Knowing $\hat{\xi}$, we calculated the drop of the neutron emission, as described by equation (27). For the beam radial distribution given by figure 3 and the plasma density profile shown in [6] we obtained $\Delta I/I = -7.0\%$. In addition, the same calculation with homogeneous plasma resulted in $\Delta I/I = -5.7\%$. We, thus, infer that in the framework of the model used (which assumes that the number of the resonant particles is conserved) the main mechanism affecting the change of the neutron emission is the velocity distortion of the energetic ion distribution function.

We remind that the experimentally observed drops of the neutron emission were larger, 10–15%. On the other hand, our model overestimates the change of the neutron emission caused by distortion of the distribution function of passing particles. The matter is that it is based on the assumption that all the injected ions are resonant and slow down due to the

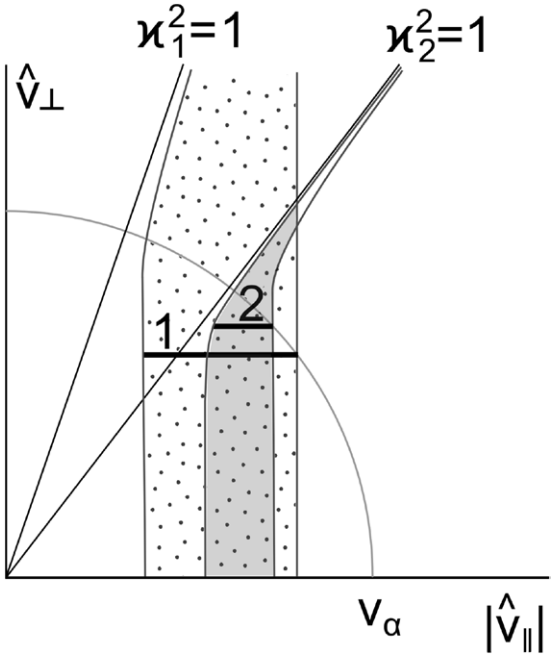

Figure 6. Sketch showing two resonance regions (shaded) and two plateau regions, i.e. the regions with $\partial f_b/\partial\hat{v}_\parallel = 0$, for the beam ions in DIII-D (bold horizontal lines): first, for well passing particles (located at some radius r_1), and second, for marginally passing ones (at $r_2 > r_1$). It was assumed that the particles slow down due to E-GAM instability. The separatrix $\kappa_p^2 \equiv \hat{v}_\parallel^2/(2\epsilon\,\hat{v}_\perp^2) = 1$ is the boundary between the regions of the toroidally trapped particles and the passing ones, $\kappa_1 \equiv \kappa_p(r_1)$ and $\kappa_2 \equiv \kappa_p(r_2)$. The circle approximates the fast-ion birth velocity ($v^2 \approx \hat{v}_\parallel^2 + \hat{v}_\perp^2$). The well passing particles and the marginally passing particles are redistributed along the lines labelled by '1' and '2', respectively. We observe that the marginally passing particles approach the separatrix vicinity, in contrast to the well passing particles.

instability. One can conclude from here that, probably, orbit transformations and the concomitant loss of some injected ions with $\kappa_p \approx 1$ indeed took place in the experiment, enhancing drops of the neutron emission. This conclusion agrees with experimental observations of fast-ion losses during E-GAM and results of numerical simulations, see [8].

4. Summary and conclusions

The obtained results and conclusions can be summarized as follows.

GAM / E-GAM modes lead to slowing down of the injected passing ions destabilizing these modes. The slowing down (described by equations (21) and (22)) can be significant due to large amplitude of the density perturbations, such as that observed in DIII-D experiments (where $\hat{n}_e/n_0 \gtrsim 1\%$).

Because GAM / E-GAM conserves the canonical angular momentum, the process of slowing down of the injected ions destabilizing the mode leads to radial displacements of these ions up to a distance about their poloidal Larmor radius ($\rho_{\rm pol}$), the maximum effect taking place when the resonance width in velocity space is large ($\Delta v_\parallel^{\rm res} \lesssim v_\parallel^i$). This implies that in the ITER-size machines, even in the case of strong cooling of the energetic ions, their radial displacements will be much less than the plasma radius and play hardly any role. In contrast to this, in modern tokamaks, where $\rho_{\rm pol} \lesssim a$, the GAM-produced displacements of injected ions can lead to noticeable effects.

The resonance width in GAMs is actually the width of the resonance island around the exact resonance $\omega = |\omega_t|$. In the case of E-GAM (when $\omega = \omega_t$), the period of the particle drift motion inside the island ($\tau_{\rm isl}$) is connected to the mode frequency (f, in Hz) by a simple relation $\tau_{\rm isl} = 4f^{-1}v_\parallel^i/\Delta v_\parallel^{\rm res}$. For instance, for $v_\parallel^i/\Delta v_\parallel^{\rm res} = 5$ and $f = 20$–50 kHz we have $\tau_{\rm isl} = 1$–0.4 ms. This time can be less than the instability burst duration and the characteristic collisional times, in which case the instability forms a plateau in the phase space of the energetic ions. This, in turn, may affect the instability.

Surprisingly, the expressions for the frequency of the particle motion inside the island, i.e. the frequency of superbanana motion, and the resonance width (but not for the transit frequency) of the well-passing particles turned out to be valid with a good accuracy also for the marginally passing ones. The exception is the case when the particle trapping parameter, κ_p, is extremely close to unity ($\omega_{\rm isl} \to \infty$ and $\Delta\mathcal{E}^{\rm res} \to 0$ for $\kappa_p \to 1$).

This result is of importance because marginally passing particles can be resonant with GAM and, especially, with E-GAM having lower frequency than the GAM frequency. In particular, the frequency of the E-GAM mode in the DIII-D experiment was less than the GAM frequency by a factor of two [6]. In this experiment, mainly marginally passing particles were affected by instability bursts, which resulted in drops of the neutron emission produced by the D–D beam-plasma reaction.

Equations describing the change of the beam-plasma fusion yield due to the velocity distortion and radial displacement of energetic ions due to a GAM / E-GAM mode were derived. It was shown that the formation of a plateau in the velocity distribution can be the main factor leading to drops of the neutron emission. Using a simple model, the influence of E-GAM on the neutron emission in the DIII-D experiment reported in [6] was considered. This model employed the fact that the E-GAM activity took place shortly after the beginning of NBI, so that the effects of collisional slowing down on the equilibrium distribution function of the injected ions were negligible. The model predicts that the drops of the neutron emission cannot exceed 7%, which is less than 10–15% observed experimentally. This indicates that the orbit transformation and, possibly, the concomitant particle loss caused by E-GAM—the factors ignored in our model—played an important role in the change of the neutron emission. The physics of orbit transformation is not quite clear. The matter is that the Coulomb pitch-angle scattering time was very large, $\tau_\perp \sim 1$ s, whereas the instability burst duration was only $\sim$1 ms, and, furthermore, the neutron emission started to drop at the beginning of the instability burst, i.e. well before the mode amplitude became maximum (see figure 1 of [6]). For this reason only particles born very close to the separatrix between the toroidally trapped particles and passing particles would undergo the orbit transformation caused by Coulomb pitch-angle scattering. However, the number of these particles

seems negligible. A possible explanation then is that the particles approach the separatrix due to their motion along the island in the $(\mathcal{E}, r, \theta)$ space; then they cross the separatrix either due to collisions or in a collisionless way. The physics of the latter is similar to that of the transformation of transitioning particles from the locally trapped state to the locally passing state in stellarators [21]. This two-stage process agrees with the picture shown in figure 4 of [8], where a passing 75 keV ion moves outwards and is eventually transformed into a trapped particle.

Note that if a global GAM mode in a plasma with energetic ions could be excited by antennae, the energetic particles would be accelerated and the fusion reaction rate would increase.

Acknowledgments

This work was supported in part by the Project No. 6058 of the Science and Technology Center in Ukraine and the National Academy of Sciences of Ukraine (NASU) and the Project No. 0114U000678 of NASU.

Appendix A. Hamiltonian approach to the study of motion of passing particles resonant with low-frequency perturbations

We begin with deriving general expressions for the width of a resonance island and the frequency of motion in the island (superbanana motion). We restrict ourselves to resonances of passing particles with low-frequency modes, for which we can neglect the perturbation of B and cyclotron resonances. In addition, we assume that the resonant islands are not too wide and, thus, do not overlap. Afterwards, we elaborate these expressions by finding the rate of the energy exchange between passing particles and GAM due to the resonance $\omega = |\omega_t|$.

We proceed from the guiding-centre Lagrangian differential form [22] presented in terms of action–angle variables [23]:

$$\Gamma = J_\phi \,\mathrm{d}\phi + J_\vartheta \,\mathrm{d}\vartheta - \mathcal{E}\,\mathrm{d}t + \frac{e}{c}\tilde{A}_\phi \,\mathrm{d}\phi + \frac{e}{c}\tilde{A}_\vartheta \,\mathrm{d}\vartheta - e\tilde{\Phi}\,\mathrm{d}t, \tag{A.1}$$

where J_ϕ and J_ϑ are the toroidal and poloidal actions of the motion in the absence of the wave, ϕ and ϑ are the respective canonically conjugate angles, $\mathcal{E} = \mathcal{E}(J_\vartheta, J_\phi)$ is the kinetic energy of the particle, t is time, $\tilde{A}_\phi$ and $\tilde{A}_\vartheta$ are the contravariant components of the wave vector potential, and $\tilde{\Phi}$ is the wave scalar potential. When writing (A.1), we have discarded the variables describing the cyclotron motion and the terms containing the perturbation of B. The coordinate transformation $J_\phi = \bar{J}_\phi - (e/c)\tilde{A}_\phi$, $J_\vartheta = \bar{J}_\vartheta - (e/c)\tilde{A}_\vartheta$ gives a possibility to describe the wave effect in terms of a single quantity:

$$\Gamma = \bar{J}_\phi \,\mathrm{d}\phi + \bar{J}_\vartheta \,\mathrm{d}\vartheta - \mathcal{E}(\bar{J}_\vartheta, \bar{J}_\phi)\,\mathrm{d}t + V\,\mathrm{d}t, \tag{A.2}$$

where we have omitted the terms of second order in the wave amplitude,

$$V = -e\tilde{\Phi} + \frac{e}{c}\omega_\phi \tilde{A}_\phi + \frac{e}{c}\omega_\vartheta \tilde{A}_\vartheta \tag{A.3}$$

is the effective potential energy of the wave, $\omega_\phi = \partial\mathcal{E}/\partial J_\phi$ and $\omega_\vartheta = \partial\mathcal{E}/\partial J_\vartheta$ are the frequencies of the orbital motion. One can see that the differential form (A.2) describes a Hamiltonian system with the coordinates ϑ and ϕ, the momenta $\bar{J}_\vartheta$ and $\bar{J}_\phi$, and the Hamiltonian

$$H(\bar{J}_\vartheta, \bar{J}_\phi, \vartheta, \phi, t) = \mathcal{E} - V. \tag{A.4}$$

Below we omit bars over J_ϕ and J_ϑ (which does not affect the particle motion to first order in the wave amplitude).

Now we expand V in Fourier series in canonical angles:

$$V = \mathrm{Re}\sum_s V_{sn}(J_\vartheta, J_\phi)\exp(-\mathrm{i}\omega t + \mathrm{i}s\vartheta - \mathrm{i}n\phi), \tag{A.5}$$

where

$$V_{sn} = \oint \frac{\mathrm{d}\vartheta\,\mathrm{d}\phi}{2\pi^2} V \exp(\mathrm{i}\omega t - \mathrm{i}s\vartheta + \mathrm{i}n\phi), \tag{A.6}$$

and the integration is performed along unperturbed orbits ($J_\vartheta = \mathrm{const}$, $J_\phi = \mathrm{const}$). The coefficients V_{sn} (matrix elements of the wave–particle interaction) characterize the intensity of the resonant interaction between the particles and the wave at the corresponding resonances

$$\Omega_{sn}(J_\vartheta, J_\phi) \equiv s\omega_\vartheta - n\omega_\phi - \omega = 0. \tag{A.7}$$

When $\omega \neq 0$, we can express each matrix element at the corresponding exact resonance in terms of $\tilde{\boldsymbol{E}}$. Combining equations (A.3), (A.6) and (A.7) and integrating by parts, we find

$$\begin{aligned} V_{sn} &= \frac{e}{\omega}\oint \frac{\mathrm{d}\vartheta\,\mathrm{d}\phi}{2\pi^2}\left[\omega_\vartheta\left(\frac{\omega}{c}\tilde{A}_\vartheta - s\tilde{\Phi}\right)\right. \\ &\quad \left. + \omega_\phi\left(\frac{\omega}{c}\tilde{A}_\phi + n\tilde{\Phi}\right)\right]\exp(\mathrm{i}\omega t - \mathrm{i}s\vartheta + \mathrm{i}n\phi) \\ &= \oint \frac{\mathrm{d}\vartheta\,\mathrm{d}\phi}{2\pi^2}\frac{e}{\mathrm{i}\omega}(\boldsymbol{v}_0\cdot\tilde{\boldsymbol{E}})\exp(\mathrm{i}\omega t - \mathrm{i}s\vartheta + \mathrm{i}n\phi), \end{aligned} \tag{A.8}$$

with $\boldsymbol{v}_0$ the unperturbed velocity of the particles. Let us define the quantity

$$Z = \frac{e}{\omega}(\boldsymbol{v}_0\cdot\tilde{\boldsymbol{E}}) = \mathrm{Re}\sum_s Z_{sn}\exp(-\mathrm{i}\omega t + \mathrm{i}s\vartheta - \mathrm{i}n\phi). \tag{A.9}$$

It follows from (A.8) that at the resonance $V_{sn} = Z_{sn}/\mathrm{i}$. Hence, averaging equation (A.9) in time along a resonant unperturbed trajectory, we obtain

$$|V_{sn}| = |Z_{sn}| = \max\frac{e}{\omega}\langle\boldsymbol{v}_0\cdot\tilde{\boldsymbol{E}}\rangle, \tag{A.10}$$

where 'max' means maximization in the wave phase.

Let us consider the vicinity of a single resonance given by (A.7), retaining only the resonant harmonic in equation (A.6). The equations of motion resulting from the Hamiltonian (A.4) show that small particle deviations from the resonance satisfy the relationship

$$\frac{\Delta\mathcal{E}}{\omega} = -\frac{\Delta J_\vartheta}{s} = \frac{\Delta J_\phi}{n}. \tag{A.11}$$

Now we transform the coordinates in order to exclude the time dependence from the perturbation. For example, if $s \neq 0$,

we can introduce the variable $\alpha = \vartheta - (n/s)\phi - (\omega/s)t$ instead of ϑ. Then the new Hamiltonian is

$$\hat{H}(\hat{J}_\alpha, \hat{J}_\phi, \alpha, \phi) = \hat{H}_0(\hat{J}_\alpha, \hat{J}_\phi) - \mathrm{Re}[V_{\mathrm{sn}} \exp(\mathrm{i}s\alpha)]$$
$$= \mathcal{E} - (\omega/s)J_\vartheta - \mathrm{Re}[V_{\mathrm{sn}} \exp(\mathrm{i}s\alpha)] \quad (A.12)$$

with $\hat{J}_\alpha = J_\vartheta$ and $\hat{J}_\phi = J_\phi + (n/s)J_\vartheta$. This Hamiltonian does not depend on ϕ; therefore, the canonical coordinate pair $(\hat{J}_\phi, \phi)$ is an ignorable degree of freedom. Now we follow a well-known technique of the nonlinear resonance theory [24]. As $\partial\hat{H}_0/\partial\hat{J}_\alpha = \Omega_{\mathrm{sn}}/s = 0$ at the resonance (A.7), we can approximate the Hamiltonian (A.12) near this resonance with a nonlinear pendulum Hamiltonian:

$$\hat{H} = Y(\Delta\hat{J}_\alpha)^2/2 + |V_{\mathrm{sn}}|\cos[s(\alpha - \alpha_0)], \quad (A.13)$$

where α_0 is determined by $\arg(V_{\mathrm{sn}})$,

$$Y = \frac{\partial^2\hat{H}_0}{\partial\hat{J}_\alpha^2} = \frac{1}{s}\left[\left.\frac{\partial\,\Omega_{\mathrm{sn}}}{\partial J_\vartheta}\right|_{\mathcal{E},\mu} - \left(\left.\frac{\partial J_\phi}{\partial J_\vartheta}\right|_{\mathcal{E},\mu} + \frac{n}{s}\right)\omega_\phi \left.\frac{\partial\,\Omega_{\mathrm{sn}}}{\partial\mathcal{E}}\right|_{J_\vartheta,\mu}\right]. \quad (A.14)$$

Assuming that $|V_{\mathrm{sn}}| \approx \mathrm{const}$, we use the conservation of $\hat{H}$ to find the widths of the resonance island in J_ϑ and energy:

$$\Delta\mathcal{E}^{\mathrm{res}} = (\omega/|s|)\Delta J_\vartheta^{\mathrm{res}} = 4(\omega/|s|)|V_{\mathrm{sn}}/Y|^{1/2}. \quad (A.15)$$

The frequency of motion around the island centre ('superbanana frequency') can also be found from (A.13):

$$\omega_{\mathrm{isl}} = s|V_{\mathrm{sn}}Y|^{1/2}. \quad (A.16)$$

Now we calculate Y for passing particles, assuming that $\rho/r \ll 1$, $\epsilon \ll 1$. In this case, the following approximations are justified:

$$J_\vartheta \approx (e/c)\psi_T, \quad (A.17)$$

$$\frac{\partial J_\phi}{\partial J_\vartheta} = -\frac{\omega_\vartheta}{\omega_\phi} \approx -\frac{1}{q}, \quad (A.18)$$

$$\omega_\phi \approx \frac{\pi}{2\mathbf{K}(\kappa_p^{-1})}\frac{\kappa_p v}{R_s}\sqrt{2\epsilon\lambda}, \quad (A.19)$$

Putting these expressions into equation (A.14) and using (A.7), we obtain:

$$Y = \frac{\omega^2}{Mv^2s^2}U\Xi \quad (A.20)$$

with

$$\Xi = 1 - \frac{\rho v\omega_\phi s}{\kappa_e r^2\omega^2 q}\left[\frac{s\hat{s}}{U} + \frac{s - nq}{2}(U^{-1} - 1 + \lambda)\right], \quad (A.21)$$

$$U = \frac{\mathbf{E}(\kappa_p^{-1})}{\mathbf{K}(\kappa_p^{-1})}\frac{1}{2\epsilon\lambda(\kappa_p^2 - 1)} \quad (A.22)$$

Substituting equation (A.20) for Y in (A.15) and (A.16), we find

$$\Delta\mathcal{E}^{\mathrm{res}} = 4v|MV_{\mathrm{sn}}/(U\Xi)|^{1/2}, \quad (A.23)$$

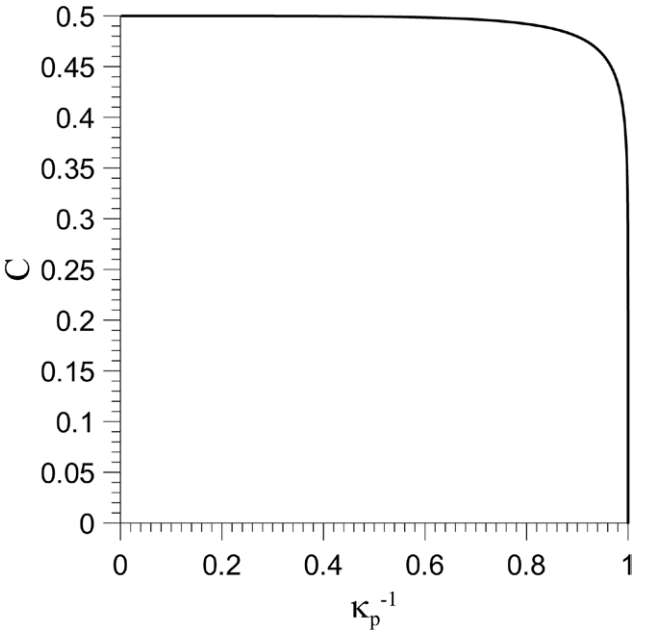

Figure A1. The function $C(x)$ given by equation (A.33).

$$\omega_{\mathrm{isl}} = (\omega/v)|V_{\mathrm{sn}}U\Xi/M|^{1/2}. \quad (A.24)$$

When the particles are well passing in the sense that the $v_\parallel$ weakly oscillates along the unperturbed orbits ($\lambda \ll 1$), the above expressions can be simplified. In this case,

$$U \approx (1 - \lambda)^{-1} \approx v^2/v_\parallel^2 \quad (A.25)$$

and we find, in agreement with [25],

$$\Delta\mathcal{E}^{\mathrm{res}} = 4|v_\parallel|\sqrt{M|V_{\mathrm{sn}}/\Xi|}, \quad (A.26)$$

$$\omega_{\mathrm{isl}} = \frac{|s - nq|}{qR_s}|V_{\mathrm{sn}}\Xi/M|^{1/2}, \quad (A.27)$$

$$\Xi = 1 - q\hat{s}\frac{\rho_\parallel R_s}{\kappa_e r^2}\frac{s^2}{(s - nq)^2}. \quad (A.28)$$

Note that the two terms of equation (A.28) correspond to two mechanisms of detuning of the particles from the resonance: the energy change and the change of q. It is possible that these two terms mutually cancel, resulting in $\Xi \approx 0$. To find the resonance width in this case, we need to take into account cubic terms in (A.13) and, possibly, approximations of higher order in ε and ρ/r instead of (A.17)–(A.19). Our estimates for well passing particles show that the cubic terms are negligible when $|\Xi| \gg \hat{s}\Delta r^{\mathrm{res}}/r$, where Δr^{res} is the radial width of the resonance island. Thus, equations (A.23) and (A.24) are valid only when $|\Xi| \gg \max\{\hat{s}\Delta r^{\mathrm{res}}/r, \epsilon, \rho/r\}$. We have not made a similar but more cumbersome analysis for marginally passing particles.

We proceed by calculating the magnitude of $|V_{\mathrm{sn}}|$ for the resonances $(s, n) = (\pm 1, 0)$ with GAM. The GAM consists of two components: transversal motion of the plasma (mainly with $m = 0$) and longitudinal motion (mainly with $m = \pm 1$), both capable of being in the $(\pm 1, 0)$ resonance with passing particles. Now we estimate the contributions of these

components to the matrix elements separately. We will consider only $|V_{10}|$ (because $|V_{-1,0}|$ is the same).

The contribution of the transversal component to this matrix elements (which we denote $|V_{10}^{\perp}|$) comes mainly from the $(m,\ n) = (0,\ 0)$ harmonic of the wave potential (it follows from the consideration in [26] that the $\Phi_{20} \sim \beta q^2 \Phi_{00}$ is small even when the plasma cross-section is elongated; here and below the subscript 'mn' at a quantity refers to the $(m,\ n)$ Fourier harmonic of the perturbation). We obtain from (A.10):

$$|V_{10}^{\perp}| = \max_{t_0}\left\{\frac{e}{\omega}\frac{\Phi_{00}' v_{\mathrm{D}}}{\kappa_{\mathrm{e}}} \oint \frac{\mathrm{d}t}{\tau_t}\ \sin(\omega t)\sin\theta\right\}, \tag{A.29}$$

where $t_0 = t|_{\theta=0}$, the integrals are taken over one poloidal transit along unperturbed resonant orbits, 'prime' denotes the radial derivative. When writing this equation, we have neglected the variation of v_{D} along the orbit and took into account that the canonical angle ϑ satisfies $\dot{\vartheta} = \omega_\vartheta = \mathrm{const}$. Note that the poloidal angle θ in (A.29) (and throughout the main text of the article) is a flux coordinate, which is *not* a linear function of time, especially for weakly passing particles.

To calculate the integral appearing in (A.29), we notice that when $\rho/r \ll 1$ and $\epsilon \ll 1$, the unperturbed motion of the passing particles is reduced to the pendulum Hamiltonian:

$$H_p = \mathcal{E} - \mu\bar{B} = P^2/(2Mq^2R_s^2) + \epsilon\mu\bar{B}\cos\theta, \tag{A.30}$$

where $P = Mv_{\parallel}qR_s$. The equation of passing trajectories of the pendulum is known (see, e.g. [24, 27]):

$$\begin{aligned}\sin\theta &= \sin\{2\,\mathrm{am}[\omega_r(t-t_0), \kappa_p^{-1}]\}\\ &= 2\,\mathrm{sn}[\omega_r(t-t_0), \kappa_p^{-1}]\,\mathrm{cn}[\omega_r(t-t_0), \kappa_p^{-1}],\end{aligned} \tag{A.31}$$

where $\omega_r = \kappa_p v/(qR_s)\sqrt{\epsilon\lambda/2}$, am, cn and sn are Jacobian elliptic functions (amplitude, cosine and sine, respectively). Putting equation (A.31) into (A.29) and using the Fourier expansions of cn and sn [27], we obtain

$$|V_{10}^{\perp}| = C(\kappa_p^{-1})\frac{v_{\mathrm{D}}}{\kappa_{\mathrm{e}}\omega}|e\Phi_{00}'|, \tag{A.32}$$

where

$$C(\kappa_p^{-1}) = \frac{2\pi^2}{x^2\mathbf{K}^2(x)} \times\left\{\frac{\mathbf{q}(x)}{1-\mathbf{q}^2(x)} - \sum_{j=0}^{\infty}\frac{[1-\mathbf{q}^2(x)]\mathbf{q}^{4j+3}(x)}{[1-\mathbf{q}^{4j+2}(x)][1-\mathbf{q}^{4j+6}(x)]}\right\}\Bigg|_{x=\kappa_p^{-1}}, \tag{A.33}$$

$\mathbf{q}(x) = \exp[-\pi\mathbf{K}(\sqrt{1-x^2})/\mathbf{K}(x)]$. The function $C(x)$ turns out to be almost constant over the most part of the interval $0 \leqslant x < 1$, see figure A1. Thus, we can take

$$C \approx 1/2. \tag{A.34}$$

with error less than 10% except for marginally passing particles with $\kappa_p - 1 < 0.034$.

The electric field harmonic associated with the acoustic (longitudinal) component of GAM cannot be found in the framework of ideal MHD. To calculate it, we use the fact that the electron density obeys the Boltzmann law along a field line, which yields

$$\Phi_{10} = -\frac{T_{\mathrm{e}}}{e_{\mathrm{e}}}\frac{n_{10}}{n} = \frac{T_{\mathrm{e}}}{e_{\mathrm{e}}}\zeta_{10}, \tag{A.35}$$

where $\zeta = \nabla\cdot\boldsymbol{w}$, $\boldsymbol{w}$ is the hydrodynamic velocity of the plasma, T_{e} and e_{e} are the electron temperature and charge, respectively. Using the equation

$$(\omega^2 + c_s^2\nabla_{\parallel}^2)\tilde{\zeta} - \frac{2\mathrm{i}c\omega}{B^2}(\boldsymbol{B}\times\boldsymbol{\mathcal{K}})\cdot\nabla\tilde{\Phi} = 0, \tag{A.36}$$

(see, e.g. [11, 13]), where $\boldsymbol{\mathcal{K}}$ is the field line curvature, we express ζ_{10} in terms of Φ_{00}' and find that the contribution of Φ_{10} to V_{10} is

$$|V_{10}^{\parallel}| = \max\frac{e}{\omega}\left\langle v_{\parallel}\Phi_{10}/(qR_s)\right\rangle = \frac{ZcT_{\mathrm{e}}}{B\omega R_s\mathcal{S}\kappa_{\mathrm{e}}}|\Phi_{00}'|, \tag{A.37}$$

with Z the fast ion charge number.

Comparing $|V_{10}^{\perp}|$ and $|V_{10}^{\parallel}|$, we observe that $V_{10}^{\perp}$ dominates:

$$|V_{10}^{\parallel}|/|V_{10}^{\perp}| = ZT_{\mathrm{e}}/(\mathcal{E}\mathcal{S}). \tag{A.38}$$

Taking $s = 1$, $n = 0$ and $\Xi = 1$, substituting (A.32) and (A.34) for $|V_{10}|$ in (A.26) and (A.27) and using the resonance condition $v_{\parallel} = qR_s\omega$, we arrive at equations (17) and (18). Similarly, equations (40) and (41) follow from equations (A.24) and (A.23), respectively, if we use the relationship $v_{\parallel}^2(\pi) = 2\epsilon\lambda(\kappa_p^2 - 1)v^2$ and assume that $\rho R_s/r^2 \ll 1$ (and, thus, $\Xi \approx 1$).

Appendix B. Linear and nonlinear GAM resonances

The analysis in this work is carried out in the assumption that the energetic ions interact with the GAM / E-GAM mode by means of the resonance $\omega = |\omega_t|$. However, this is not the only possible resonance. Below we consider other GAM resonances and discuss their role.

First of all, we note that the final orbit width of the particles leads to additional resonances [28]. In the case of perturbations with $m = n = 0$, these resonances are given by

$$\omega = p|\omega_t|, \tag{B.1}$$

where $p = 2, 3, 4, \ldots$. These resonances involve particles with lower energies compared to those of the resonance with $p = 1$ ($\mathcal{E}_{\parallel}^{\mathrm{res}}(p>1) = \mathcal{E}_{\parallel}^{\mathrm{res}}(p=1)/p^2$). In addition, when the well passing ions have the resonant energy $\mathcal{E}_{\parallel}^{\mathrm{res}}(p>1) \ll \mathcal{E}_{\alpha}$, the $p > 1$ resonances provide the interaction of the mode with the marginally passing particles (with $\kappa_p \to 1$) of high energy, $\mathcal{E} \sim \mathcal{E}_{\alpha}$. Therefore, in the presence of particles interacting with the mode through the $p = 1$ resonance, the $p > 1$ resonances weakly contribute to the instability growth rate, but they can lead to stochastic motion near the separatrix $\kappa_p = 1$.

When the mode amplitude is so large that it considerably affects the particle orbits, the resonances with $p < 1$ arise. This can be easily seen from the equation for $\dot{\mathcal{E}}$ which determines the change rate of the particle energy. In section 2, the integral in equation (3) for $\langle\dot{\mathcal{E}}\rangle$ was calculated with neglecting

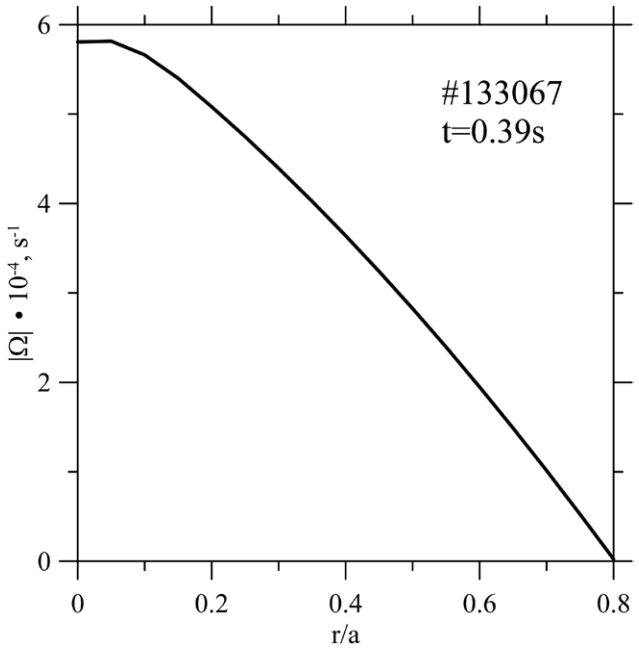

Figure C1. Frequency of the toroidal rotation in DIII-D.

the mode electric field in the equation for $\theta(t)$. Now we calculate the same integral, but with the use of a more exact equation for $\theta(t)$. Restricting ourselves to consideration of a well passing particle with a standard orbit, we obtain from equation (1) for $\dot{\theta}$:

$$\theta(t) = \omega_t t - \frac{\omega_E}{\omega}\cos\omega t + \theta_0(t), \tag{B.2}$$

where $\theta_0(t)$ is a slowly varying function, its dependence on t comes from the change of ω_t during the particle motion. Taking $\omega_E/\omega \ll 1$, we can write $\sin\theta \approx \sin(\omega_t t + \theta_0) - (\omega_E/\omega)\cos(\omega_t t + \theta_0)\cos\omega t$. Then $\langle\dot{\mathcal{E}}\rangle = -e\hat{E}v_{\mathrm{D}}J/\kappa_{\mathrm{e}}$, with

$$J = \oint \frac{\mathrm{d}t}{\tau_t}\sin\theta\sin\omega t$$
$$= \oint \frac{\mathrm{d}t}{\tau_t}\left[\sin\omega t\sin(\omega_t t + \theta_0) - \frac{\omega_E}{2\omega}\sin 2\omega t\cos(\omega_t t + \theta_0)\right], \tag{B.3}$$

Here the first term does not vanish due to the resonance $\omega = \omega_t$, being maximum at $\theta_0 = 0$, whereas the second term does not vanish due to the resonance $2\omega = \omega_t$ (i.e. the $p = 1/2$ resonance), being maximum at $\theta_0 = \pi/2$. Using equation (B.3) we obtain the energy change rate due to the $p = 1/2$ resonance as follows:

$$\langle\dot{\mathcal{E}}\rangle = -\frac{1}{2}e\hat{E}\omega_E\Delta_r\sin\theta_0, \tag{B.4}$$

where $\Delta_r = v_{\mathrm{D}}/(|\omega_t|\kappa_{\mathrm{e}})$ is the orbit half-width. This is less than the energy change rate due to the linear resonance by a factor of $\omega_E/(2\omega)$.

Let us evaluate the ratio $\omega_E/(2\omega)$. Taking into account that [11]

$$|\hat{E}| = \omega B\kappa_{\mathrm{e}}R_s\mathcal{S}\frac{1}{c}\frac{\hat{n}}{n_0}, \tag{B.5}$$

we obtain

$$\frac{\omega_E}{2\omega} = \frac{\mathcal{S}}{2\epsilon}\frac{\hat{n}}{n_0}. \tag{B.6}$$

We observe that the ratio $\omega_E/(2\omega)$ does not depend on the mode frequency.

According to [6], $\hat{n}/n_0 = 1.5\%$; hence, we obtain $\omega_E/(2\omega) = 0.03$ at $r = a/2$ for the DIII-D experiment. Thus, the rate of the energy change due to the $p = 1/2$ resonance is much less than that due to the linear resonance. The width of the island produced by this resonance can be estimated as $\Delta\mathcal{E}^{\mathrm{res}}_{p=1/2} \sim \sqrt{\omega_E/(2\omega)}\,\Delta\mathcal{E}^{\mathrm{res}}_{p=1} = 0.17\Delta\mathcal{E}^{\mathrm{res}}_{p=1}$.

This result was obtained in lowest order in $\omega_E/(2\omega)$. Proceeding to higher orders, one could obtain resonances for other rational values of p. Note that orbit averaging of $\dot{\mathcal{E}}$ in this case requires, generally speaking, integration over several transit periods. The higher order resonances lead to smaller energy change rates and more narrow island widths. Detailed study of these resonances was carried out in [29].

It is clear that the $p < 1$ resonances do not affect the growth rate at the initial stage of the instability. They involve different groups of particles into the interaction with the mode. Therefore, it is not clear *a priori* whether they enhance or weaken the instability at high mode amplitudes. Compared to the linear resonance, the $p < 1$ resonances are characterized by much smaller widths, unless the mode amplitude is extremely large, in which case they can lead to stochastic motion of particles.

Appendix C. The influence of the plasma temperature and toroidal rotation on the fusion reaction rate

The neutron emission resulting from the beam-plasma fusion reactions depends on distribution functions of both the beam and the plasma. When the beam energy well exceeds the plasma temperature, the relative velocity of two colliding ions, $\boldsymbol{u} \equiv \boldsymbol{v}_b - \boldsymbol{v}_p$, approximately equals to the beam ion velocity ($\boldsymbol{v}_p$ is the velocity of a plasma ion). This implies that details of the plasma distribution function play a minor role, so that this function can be approximated as $F_p(\boldsymbol{v}) = n_p\delta(\boldsymbol{v})$. This approximation was used in our basic equation for the fusion reaction rate given by equation (26). In order to evaluate its accuracy, below we calculate the local fusion reaction rate, assuming that a plasma with Maxwell distribution function moves with the average velocity V,

$$F_p = n_p\left(\frac{M_p}{2\pi T}\right)^{3/2}\exp\left[-\frac{M_p v_\perp^2}{2T} - \frac{M_p(v_\parallel - V)^2}{2T}\right], \tag{C.1}$$

and that the beam distribution function is

$$F_b = n_b\frac{1}{\pi}\frac{\delta(v_\perp)}{v_\perp}\delta(v_\parallel - v_b), \tag{C.2}$$

where T is the plasma temperature, M_p is the plasma ion mass.

Using these distribution functions, we obtain from equation (25):

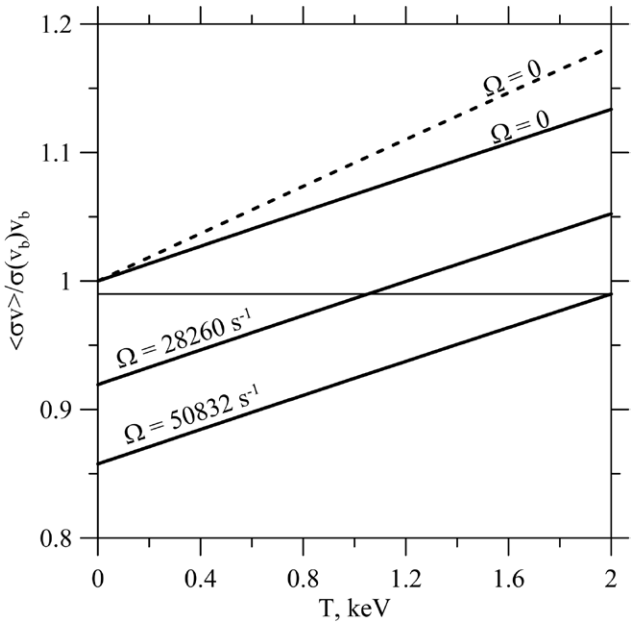

Figure C2. Effects of the plasma temperature and toroidal rotation on the rate of beam-plasma D–D reaction (neutron channel) in the case when all beam ions have the same energy, $\mathcal{E}_b = M_b v_b^2/2$. Thick lines: the ratio $\langle\sigma v\rangle/[\sigma(v_b)v_b]$ for $\mathcal{E}_b = 75$ keV and various magnitudes of Ω; Dashed line: $\langle\sigma v\rangle/[\sigma(v_b)v_b]$ for $\mathcal{E}_b = 65$ keV and $\Omega = 0$. In our calculations we took $V = R\,\Omega$ with $R = 170$ cm. The rotational speeds $\Omega = 50832$ rad s^{-1} and $\Omega = 28\,260$ rad s^{-1} correspond to the plasma rotation at $r/a = 0.2$ and $r/a = 0.5$, respectively, in the DIII-D discharge #133067, as shown in figure C1. The thin horizontal line is plotted to demonstrate that the reaction rate at $T = 2$ keV and $T = 1$ keV is approximately the same and equals to that at $T = 0$, $V = 0$ (1% less).

$$I_{\rm L} = n_b n_p \langle\sigma v\rangle, \tag{C.3}$$

where $\langle\sigma v\rangle$ is defined by

$$\mathcal{R} \equiv \frac{\langle\sigma v\rangle}{\sigma(v_b)v_b} = \frac{1}{\sqrt{\pi}} \int_0^\infty {\rm d}w\, {\rm e}^{-w} \int_{-\infty}^\infty {\rm d}y\, {\rm e}^{-y^2} \frac{\sigma(u)}{\sigma(v_b)} \frac{u}{v_b}, \tag{C.4}$$

with

$$\frac{u}{v_b} = \frac{1}{y_b}\left\{ w + \left[y_b\left(1 - \frac{V}{v_b}\right) - y \right]^2 \right\}^{1/2}, \tag{C.5}$$

$w = v_\perp^2/v_T^2$, $y = v_\parallel/v_T$, $y_b = v_b/v_T$, $v_T = \sqrt{2T/M_p}$.

Because $w \sim 1$ and $y \sim 1$ mainly contribute to the integral in equation (C.4), whereas $y_b \to \infty$ at $T \to 0$, it is clear that $u = v_b$ and, therefore, $\mathcal{R} = 1$ when $T = 0$ and $V = 0$. Finite plasma temperature increases u in the region where $(y \cdot y_b) < 0$ and decreases it in the region where $(y \cdot y_b) > 0$, which leads to $\mathcal{R} > 1$ at $V = 0$ due to strong dependence on the particle energy of D–D fusion reaction cross section at $\mathcal{E} < 100$ keV. On the other hand, plasma rotation reduces u and $\langle\sigma v\rangle$ for ${\rm sgn}(V \cdot v_b) > 0$ (which is the case when, e.g. plasma rotates due to beam injection), making $\mathcal{R} < 1$ at $T = 0$.

In the case of the GAM DIII-D experiments, ${\rm sgn}(V \cdot v_b) > 0$ (both v_b and V are negative). This implies that the effects of finite temperature and plasma rotation on $\langle\sigma v\rangle$ compete with each other in these experiments.

Normally, the rotation velocity, V, is considerably less than the thermal velocity, v_T. For instance, in DIII-D experiments $V < 10^7$ cm s^{-1} (figure C1 supports this statement; V and Ω are connected by the relation $V = R\,\Omega$, with Ω the rotational speed), whereas $v_T > 3 \times 10^7$ cm s^{-1} in the core region where $T = 1 - 2$ keV. Nevertheless, because σ strongly depends on u, the effect of the rotation can be comparable to that of the plasma temperature. Straightforward calculations confirm this, see figure C2. We observe that, as expected, $\langle\sigma v\rangle$ is a growing function of T. In particular, when $T = 2$ keV and $\Omega = 0$, $\langle\sigma v\rangle$ exceeds $\langle\sigma v\rangle_{T=0}$ by 13% at $\mathcal{E}_b = 75$ keV and even more at $\mathcal{E}_b = 65$ keV. However, the plasma rotation compensates this effect, making $\langle\sigma v\rangle_{T=2\,{\rm keV}} = \langle\sigma v\rangle_{T=0}$, with accuracy of 1%. Remarkably, due to rotation, the same magnitude of the reaction rate takes place at $T = 1$ keV when $\Omega = \Omega\,(r/a = 0.5)$. Note that, as seen from figure 2 of [6], 1 keV is the ion temperature at $r/a \approx 0.5$ and, in addition, the considered magnitudes of r/a (0.2 and 0.5) correspond to the borders of the region where the EGAM is located.

Thus, we have shown that the effects of plasma rotation and finite temperature may compensate each other, although a considerable enhancement of the reaction rate is possible in the case when the directions of the rotation and the beam are different. In the absence of rotation, $\langle\sigma v\rangle$ at $T \sim$ 1–2 keV considerably differs from that at $T = 0$. However, even in this case the $T = 0$ approximation can be sufficient for qualitative consideration of the change of the neutron emission during E-GAM instability. The matter is that the beam-ion displacement caused by E-GAM is accompanied (and caused by) a change of the ion energy, which affects the reaction rate stronger than the change of the temperature.

References

[1] Winsor N, Johnson J L and Dawson J M 1968 *Phys. Fluids* **11** 2448
[2] Jakubowski M, Fonck R J and McKee G R 2002 *Phys. Rev. Lett.* **89** 265003
[3] Zhao K J *et al* 2006 *Phys. Rev. Lett.* **96** 255004
[4] Boswell C J, Berk H L, Borba D N, Johnson T, Pinches S D and Sharapov S E 2006 *Phys. Lett.* A **358** 154
[5] Berk H, Boswell C J, Borba D, Figueiredo A C A, Johnson T, Nave M F F, Pinches S D, Sharapov S E and JET EFDA contributors 2006 *Nucl. Fusion* **46** S888
[6] Nazikian R *et al* 2008 *Phys. Rev. Lett.* **101** 185001
[7] Fu G Y 2008 *Phys. Rev. Lett.* **101** 185002
[8] Fisher R K, Pace D C, Kramer G J, Van Zeeland M A, Nazikian R, Heidbrink W W and García-Muñoz M 2012 *Nucl. Fusion* **52** 123015
[9] Fesenyuk O P, Kolesnichenko Ya I and Yakovenko Yu V 2012 *Plasma Phys. Control. Fusion* **54** 085014
[10] Kolesnichenko Ya I, Lepiavko B S and Lutsenko V V 2013 *Plasma Phys. Control. Fusion* **55** 125007
[11] Kolesnichenko Ya I, Lutsenko V V and Lepiavko B S 2014 *Phys. Lett.* A **378** 2683
[12] Kolesnichenko Ya I, Könies A, Lutsenko V V and Yakovenko Yu V 2011 *Plasma Phys. Control. Fusion* **53** 024007
[13] Fesenyuk O P, Kolesnichenko Ya I, Wobig H and Yakovenko Yu V 2002 *Phys. Plasmas* **9** 1589

[14] Kolesnichenko Ya I, Lutsenko V V, White R B and Yakovenko Yu V 2004 *Phys. Plasmas* **11** 5302
[15] Kolesnichenko Ya I 1980 *Nucl. Fusion* **20** 727
[16] Meneghini O *et al* 2015 *Nucl. Fusion* **55** 083008
[17] Lao L *et al* 1985 *Nucl. Fusion* **25** 1611
[18] Hawryluk R J 1981 An empirical approach *Physics of Plasmas Close to Thermonuclear Conditions (International School of Plasma Physics)* ed B Coppi (Oxford: Pergamon) p 19
[19] Pankin A, McCune D, Andre R, Bateman G and Kritz A 2004 *Comput. Phys. Commun.* **159** 157
[20] Kolesnichenko Ya I, Parail V V and Pereverzev G V 1992 *Reviews of Plasma Physics* vol 17, ed M A Leontovich (New York: Consultants Bureau) pp 1–192
[21] Beidler C D, Kolesnichenko Ya I, Marchenko V S, Sidorenko I N and Wobig H 2001 *Phys. Plasmas* **8** 2731
[22] Littlejohn R G 1983 *J. Plasma Phys.* **29** 111
[23] Kaufman A N 1972 *Phys. Fluids* **15** 1063
[24] Chirikov B V 1979 *Phys. Rep.* **52** 263
[25] Tyshchenko M H and Yakovenko Yu V 2015 *Probl. At. Sci. Technol.* **1**(21) 49
[26] Fesenyuk O P, Kolesnichenko Ya I and Yakovenko Yu V 2013 *Phys. Plasmas* **20** 122503
[27] Reinhardt W P and Walker P L 2015 Chapter 22: Jacobian Elliptic Functions *NIST Digital Library of Mathematical Functions* (http://dlmf.nist.gov/22)
[28] Kolesnichenko Ya I, Lutsenko V V, Weller A, Werner A, Wobig H, Yakovenko Yu V, Geiger J and Zegenhagen S 2006 *Nucl. Fusion* **46** 753
[29] Kramer G J, Chen L, Fisher R K, Heidbrink W W, Nazikian R, Pace D C and Van Zeeland M A 2012 *Phys. Rev. Lett.* **109** 035003